

Noise estimation of SDE from a single data trajectory

Munawar Ali^{*} Purba Das[†] Qi Feng[‡] Liyao Gao[§] Guang Lin[¶]

Abstract

In this paper, we propose a data-driven framework for model discovery of stochastic differential equations (SDEs) from a single trajectory, without requiring the ergodicity or stationarity assumption on the underlying continuous process. By combining (stochastic) Taylor expansions with Girsanov transformations, and using the drift function's initial value as input, we construct drift estimators while simultaneously recovering the model noise. This allows us to recover the underlying \mathbb{P} Brownian motion increments. Building on these estimators, we introduce the first *stochastic Sparse Identification of Stochastic Differential Equation (SSISDE)* algorithm, capable of identifying the governing SDE dynamics from a single observed trajectory without requiring ergodicity or stationarity. To validate the proposed approach, we conduct numerical experiments with both linear and quadratic drift–diffusion functions. Among these, the Black–Scholes SDE is included as a representative case of a system that does not satisfy ergodicity or stationarity.

Keywords: SSISDE, Sparse regression, SINDy, Risk-neutral Brownian motion, Physical Brownian motion, Stochastic Taylor expansion, Girsanov transformation, Signature model, Drift and diffusion estimate, Quadratic variation, Stratonovich and Itô SDE.

2000 AMS Mathematics subject classification: 62P05, 37M10, 60H10, 60G17, 65C30.

1 Introduction

Stochastic differential equations (SDEs) are fundamental tools for modeling systems with inherent randomness, but estimating the underlying continuous dynamics from observed discrete data remains both challenging and important. The initial development in this area was closely tied to applications in economics and finance, including [3, 51, 50, 6, 33, 34, 58, 24], among many others. A central challenge in working with stochastic differential equations (SDEs) is that, in practice, one typically only observes the process at discrete time points, while the key quantities driving the dynamics—such as the drift and diffusion coefficients or even the underlying noise—remain unknown. Recovering both the system parameters and the latent noise process from such partial information is therefore of significant theoretical and practical interest, particularly in stochastic modeling and statistical inference [44, 40].

In this paper, we study the problem of recovering the drift and diffusion functions from a high-frequency single realization of a continuous-time stochastic process $\{X_t\}_{t \geq 0}$ governed by the Itô SDE

$$dX_t = \mu(X_t)dt + \sigma(X_t)dB_t^{\mathbb{P}}, \quad (1)$$

where μ and σ denote the drift and diffusion functions, respectively, and $B^{\mathbb{P}}$ is a canonical Brownian motion under the physical measure \mathbb{P} , i.e. the filtration is generated by the X_t . Classical approaches to estimating μ and σ include kernel-based estimators [45, 29, 58], maximum likelihood methods [10, 21, 1], and local polynomial regression [27]. These methods, however, typically rely on ergodicity or stationarity of the underlying process or the availability of repeated observations. More recent developments employ tools from empirical process theory and martingale estimation to handle high-frequency data [22, 18], but these approaches still require strong structural assumptions such as stationarity, ergodicity, or multiple sample paths. These assumptions are often unrealistic in a financial context; for example, if one assumes the classical Black–Scholes model for

^{*}Department of Mathematics, Florida State University, Tallahassee, 32306; email: ma22bm@fsu.edu.

[†]Department of Mathematics, King's College London, London, UK; email: purba.das@kcl.ac.uk.

[‡]Department of Mathematics, Florida State University, Tallahassee, 32306; email: qfeng2@fsu.edu. This author is partially supported by the National Science Foundation under grant #DMS-2420029.

[§]Department of Computer Science, University of Washington, Seattle, WA 98195.

[¶]Department of Mathematics, Purdue University, West Lafayette, IN; email: guanglin@purdue.edu. This author is partially supported by the National Science Foundation (NSF) (DMS-2533878, DMS-2053746, DMS-2134209, ECCS-2328241, CBET-2347401, and OAC-2311848), and DOE Office of Science Advanced Scientific Computing Research program DE-SC0023161, and DOE–Fusion Energy Science, under grant number: DE-SC0024583.

a price path, then the price path is not ergodic. In the paper we address this problem via a data driven pathwise approach, based on a single trajectory of (1). A similar pathwise approach to extract noise from single trajectory has been explored in [2, Proposition 4.1].

On the other hand, in the absence of noise in (1), the deterministic dynamics can be analyzed in much greater detail. Particularly, the discovery of a deterministic dynamical system, obtained by setting $\sigma \equiv 0$ in equation (1),

$$\dot{\mathbf{x}}(t) = \mu(\mathbf{x}(t)), \quad (2)$$

can be formulated as a symbolic regression problem of the following form:

$$\dot{\mathbf{X}} = \Theta(\mathbf{X})\Xi, \quad (3)$$

where $\Theta(\mathbf{X})$ denotes the function library matrix composed of p candidate terms, typically including polynomials, trigonometric functions, exponentials, and sinusoidal functions. The unknown sparse matrix $\Xi = (\xi_1 \ \xi_2 \ \cdots \ \xi_n) \in \mathbb{R}^{p \times n}$ encodes the active terms and thus determines the governing dynamics. The input \mathbf{X} denotes the vector of data snapshots over the discrete time grid. The state snapshots $\mathbf{X}(t)$ are observed in discrete time instances, and their temporal derivatives $\dot{\mathbf{X}}(t)$ are obtained from data. The identification/estimation of the vector Ξ is called regression. Over the past decades, significant efforts have been devoted to data-driven model discovery. Early approaches include symbolic regression [43] for uncovering the structure of ODEs [56, 12]. Subsequent advances introduced sparse regression techniques for identifying ODEs [48, 14, 49] and PDEs [54, 65, 55] with constant coefficients, along with group sparsity and sequentially grouped threshold ridge regression to capture spatial- or temporal-dependent coefficients [63, 30, 15]. More recently, symbolic regression models [14, 61, 17] have focused on extracting analytic expressions from large datasets, offering greater interpretability. Recent developments in data-driven frameworks further include the use of rough path theory and signature methods [57], as well as sparse identification of nonlinear stochastic dynamics [13, 62]. Sparse learning has also proven highly effective in a broad range of applications in engineering, including fluid dynamics [8], plasma dynamics [38], nonlinear optics [26], mesoscale ocean closures [64], and computational chemistry [35].

However, the stochastic extension of Sparse Identification of Nonlinear Dynamics (SINDy) is highly non-trivial, due to the fact that SINDy fundamentally requires computing the temporal derivatives, which are known to be sensitive to noise. Additionally, it is also mathematically unclear on how to identify the drift μ and the underlying 'rough' noise term $B^{\mathbb{P}}$ of (1), from a single path observation on a finite time interval [59, 13, 62]. In contrast to the current literature concerning these problems, our method is data-driven, does not assume strong regularity conditions, ergodic or stationary properties of the underlying process, and also uses a single path of the SDE. Our technique also extracts the noise from the finite sample data. Our proposed new methodology combines stochastic analysis, approximation techniques, and linear regression, with the only major assumption being the knowledge of the drift coefficient at the initial time point. Building on the Itô–Stratonovich correspondence [52], we approximate the drift and diffusion terms using Taylor expansions and reformulate the SDE in terms of iterated integrals. These iterated integrals, also known as signatures in rough path theory [47, 31], have recently been developed into powerful signature models in finance [4, 20, 9, 19]. Our approach leverages Girsanov's theorem [32, 39] to transform the dynamics into a representation involving iterated integral type terms, which admit explicit computation [47, 41], and the convergence rate of such terms are well explored. Through further simplifications, inspired by the structure of the Black–Scholes model [11], we obtain a representation suitable for regression-based identification of drift, diffusion, and the underlying Brownian motion paths. Using the estimated increment of \mathbb{P} Brownian motion and the data snapshot of X , we introduce a new stochastic symbolic regression problem,

$$\arg \min_{\Xi_\sigma, \Xi_\mu} \|\Delta X - \Theta_\mu(X)\Xi_\mu \Delta t - \Theta_\sigma(X)\Xi_\sigma \Delta B_t^{\mathbb{P}}\|_2^2 + \mathcal{R}_{\alpha, \rho}(\Xi_\mu, \Xi_\sigma), \quad (4)$$

where the first loss is to fit the model, and the second promotes sparsity through regularization.

The remainder of the paper is organized as follows. Section 2 formulates the problem, introduces the proposed algorithms, and reviews the necessary background on SDEs. Section 3 develops the stochastic sparse identification of SDEs (SSISDE) framework for regression-based estimation, enabling the simultaneous recovery of the drift, diffusion, and underlying noise. Section 4 presents numerical experiments illustrating the effectiveness of the proposed method, including an application to the Black–Scholes SDE, which notably does not satisfy the ergodicity and stationary conditions.

2 Background and problem formulation

Let B be the Brownian motion defined on the canonical probability space $(\Omega, \mathcal{F}, \{\mathcal{F}\}_{t \geq 0}, \mathbb{P})$ ¹. We assume our time series data $X_{t_0}, X_{t_1}, \dots, X_{t_N}$ comes from the underlying continuous process X_t which follows a stochastic

¹We use the notation $B^{\mathbb{P}}$ to stress the underlying probability measure

differential equation (under the physical measure) of the form

$$dX_t = \mu(X_t)dt + \sigma(X_t)dB_t^{\mathbb{P}}. \quad (5)$$

Note that the underlying process (5) does not always process a unique solution for general drift (μ) and diffusion (σ) coefficients. Nonetheless, under nominal assumptions (Lipchitz continuity and linear growth) on the drift (μ) and diffusion (σ) coefficient, one can ensure the existence and uniqueness of such a solution [39, Chapter 5].

It has already been shown in [2, Proposition 4.1], that there is a unique ‘rough-smooth’ decomposition of paths with finite quadratic variation, i.e. from a single trajectory of X_t following the diffusion (5), one can uniquely decompose the path X_t into its drift component and rough integral component. The first main goal of this paper is to estimate simultaneously the underlying noise vector $(B_{t_0}^{\mathbb{P}}, B_{t_1}^{\mathbb{P}}, \dots, B_{t_N}^{\mathbb{P}})$, the drift vector $(\mu(X_{t_0}), \mu(X_{t_1}), \dots, \mu(X_{t_N}))$, and the diffusion vector $(\sigma(X_{t_0}), \sigma(X_{t_1}), \dots, \sigma(X_{t_N}))$ of (5) from a single discrete data vector $(X_{t_0}, X_{t_1}, \dots, X_{t_N})$. The second goal of the paper is to recover the symbolic function μ and σ from the above estimated vectors. Note that apriori we do not have information about the μ and σ function except for $\mu(X_0)$ and the fact that (5) has a unique (strong) solution (A sufficient condition for strong solution is (local) Lipschitz continuity of μ and σ).

Under the existence and uniqueness of solution of the SDE (5), the diffusion process of X_t given by (5) possesses the integral form

$$X_t = X_0 + \int_0^t \mu(X_s)ds + \int_0^t \sigma(X_s)dB_s^{\mathbb{P}}, \quad (6)$$

where the stochastic integral is understood in the Itô sense. The equation (6) can be rewritten such that the stochastic integral is understood in the Stratonovich sense:

$$X_t = X_0 + \int_0^t \left(\mu(X_s) - \frac{1}{2}\sigma(X_s)\sigma'(X_s) \right) ds + \int_0^t \sigma(X_s) \circ dB_s^{\mathbb{P}}. \quad (7)$$

The term $\frac{1}{2}\int_0^t \sigma(X_s)\sigma'(X_s)ds$ is known as the Itô-Stratonovich correction term or quadratic variation correction term corresponding to the SDE (6). If we set $\tilde{\mu}(X_s) := \mu(X_s) - \frac{1}{2}\sigma(X_s)\sigma'(X_s)$, then the SDE becomes

$$X_t = X_0 + \int_0^t \tilde{\mu}(X_s)ds + \int_0^t \sigma(X_s) \circ dB_s^{\mathbb{P}}. \quad (8)$$

We will solve the problem in two-fold; firstly by estimating the diffusion vector and underlying risk-neutral Brownian noise. Secondly, by applying a series of approximations to simplify the SDE, and then using regression to identify the noise (underlying physical Brownian motion) and the drift vector simultaneously as a solution to the ODE. The detailed algorithm is provided in Section 3. Below is the list of assumptions we need to derive the algorithm.

1. μ and σ are Lipschitz continuous.
2. $\mu \in C^3(\mathbb{R})$ and $\sigma \in C^4(\mathbb{R})$.
3. Assume the initial values of μ i.e. $\mu(X_0)$ is known (we do not need prior knowledge of $\sigma(X_0)$).
4. Assume the \mathbb{P} Brownian motion starts at 0 i.e. $B_0^{\mathbb{P}} = 0$. Without this assumption, the algorithm still applies; however, we can only recover the increments of the noise vector rather than the noise vector itself.

We summarise the key steps behind the algorithm below.

Step 1: Firstly, by taking the quadratic variation of the original data process X_t , we can eliminate the drift μ and the randomness $B^{\mathbb{P}}$ from the system. This enables us to estimate the diffusion vector $(\sigma(X_{t_0}), \sigma(X_{t_1}), \dots, \sigma(X_{t_{N-1}}))$, of (5). We then use Girsanov’s theorem to construct a measure \mathbb{Q} (often known as martingale /risk-neutral measure²) under which the drift in (5) disappears. i.e.

$$X_t = X_0 + \int_0^t -\frac{1}{2}\sigma(X_s)\sigma'(X_s)ds + \int_0^t \sigma(X_s) \circ dB_s^{\mathbb{Q}}. \quad (9)$$

As a consequence, the risk-neutral Brownian noise (denoted as $B^{\mathbb{Q}}$) can be calculated at time points t_0, t_1, \dots, t_{N-1} using the data and the (estimated) diffusion vector.

By using a symbolic regression (based on a preset library), we then recover the underlying diffusion function $\sigma : \mathbb{R} \rightarrow \mathbb{R}$. This allows us to directly calculate the σ' vector in **Step 5** without using finite difference methods.

²This measure \mathbb{Q} can be thought of as an artificial ‘lens’ under which the data process X_t looks like fair games

Step 2: For all $i \in \{0, \dots, N-1\}$ we use a change of variable formula to rewrite $\sigma(X_{t_{i+1}})$ as an expansion around X_{t_i} . Replacing this approximation of σ in the (Stratonovich) integral form of SDE (9) and combining the like terms to represent the SDE in terms of weighted sums of the (Stratonovich) iterated integral (often identified as signatures) for the $B^{\mathbb{Q}}$ up to order two³, we identify the weights.

Step 3: We approximate both the drift and diffusion coefficients $\mu(X_{t_{i+1}}), \sigma(X_{t_{i+1}})$ by a second-order Taylor expansion around (X_{t_i}) and replace the approximation into (8). This way we can represent the SDE (8) in terms of weighted sums of the (Stratonovich) iterated integral wrt the $B^{\mathbb{Q}}$ up to order two, and we identify the weights.

Step 4: We now apply the Girsanov theorem to transform our approximated SDE in **Step 3** into an approximated SDE written as a sum of weighted (Stratonovich) iterated integral with respect to the martingale Brownian motion $B^{\mathbb{Q}}$ up to order two.

Step 5: For each time interval $[t_i^n, t_{i+1}^n]$ by comparing the weights from **Step 2** and **Step 4**, we write μ as a solution of ODE where the coefficients of the ODE are written using σ, σ' and the weights from **Step 2**.

Step 6: We use a regression method to solve the weights from **Step 3** to identify the coefficients of the ODE in **Step 5**. Finally, we use an ODE solver on the time grid (t_1, \dots, t_N) to identify the drift vector $(\mu(X_{t_0}), \mu(X_{t_1}), \dots, \mu(X_{t_N}))$ and recover the increments of the physical Brownian motion $\{\Delta B_{t_i}^{\mathbb{P}} := B_{t_{i+1}}^{\mathbb{P}} - B_{t_i}^{\mathbb{P}}\}_{i=1}^{N-1}$.

Step 7: We propose *Stochastic Sparse Identification of Stochastic Differential Equation* (SSISDE) to recover the exact symbolic form of the SDE that

$$dX_t = \mu(X_t)dt + \sigma(X_t)dB_t^{\mathbb{P}}. \quad (10)$$

We introduced a stochastic symbolic regression problem inspired by SINDy, which allowed us to obtain the precise functional form of the SDE by optimizing the following target

$$\arg \min_{\Xi_{\sigma}, \Xi_{\mu}} \sum_{i=1}^N \|\Delta X_{t_i} - \Theta(X_{t_i})\Xi_{\mu} \Delta t_i - \Theta(X_{t_i})\Xi_{\sigma} \Delta B_{t_i}^{\mathbb{P}}\|_2^2 + \mathcal{R}_{\alpha, \rho}(\Xi_{\mu}, \Xi_{\sigma}), \quad (11)$$

where $\Theta(X_{t_i})$ is a library of functions (pre-)specified by the users, which commonly includes polynomials and Fourier functions. This concludes our algorithm to identify the stochastic governing equation from noisy, stochastic, and single-shot time-series observations.

3 Main Results

In this section, we introduce the main algorithm. The key idea is to formulate the estimator of the drift function as the solution of an ODE, which in turn enables the recovery of the underlying physical Brownian motion $B^{\mathbb{P}}$ given one single trajectory observation of the state process X_t on a finite time interval $[0, T]$.

Step 1: recovering \mathbb{Q} -Brownian motion. Recast the Itô SDE (5) with stating time s (may or may not be 0) and terminal time $t > s$ below,

$$X_t = X_s + \int_s^t \mu(X_u)du + \int_s^t \sigma(X_u)dB_u^{\mathbb{P}}. \quad (12)$$

By applying Girsanov's theorem, the above SDE can be represented as a martingale with respect to the \mathbb{Q} -Brownian motion $B^{\mathbb{Q}}$, which has the following form

$$X_t = X_s + \int_s^t \sigma(X_u)dB_u^{\mathbb{Q}} \quad (13)$$

where $B^{\mathbb{Q}}$ is the Brownian motion under the martingale measure \mathbb{Q} , which is often referred to risk-neutral measure in finance [36], following the dynamic

$$\forall u \in [s, t]; \quad dB_u^{\mathbb{Q}} = dB_u^{\mathbb{P}} + \frac{\mu(X_u)}{\sigma(X_u)}du, \quad (14)$$

By definition, the underlying limiting quadratic variation of process X along a given sequence of time-grid $\pi := \{\pi^N\}_{N=0}^{\infty} := \{0 = t_0^N < t_1^N < \dots < t_i^N < \dots < t_{\#(\pi^N)}^N = t\}_{N=0}^{\infty}$ with vanishing mesh (i.e. $|t_{i+1}^N - t_i^N| \xrightarrow{N \rightarrow \infty}$

³By order two we mean the error terms are of order $|t_{i+1}^n - t_i^n|^{2-\epsilon}$ for any given $\epsilon > 0$.

0), denoted by $[X]_{\pi,t} := \lim_{n \rightarrow \infty} \sum_{\pi^n \cap [0,t]} (X(t_{i+1}^n) - X(t_i^n))^2$, has the following form

$$d[X]_{\pi,t} = (\sigma(X_t))^2 dt. \quad (15)$$

By using the high frequency estimate of quadratic variation along the time-grid π^M for a given M large enough (i.e. $[X]_{\pi^M,t} := \sum_{\pi^M \cap [0,t]} (X(t_{i+1}^M) - X(t_i^M))^2$), we first obtain an estimate of σ as follows.

$$(\sigma(X_t))^2 \approx \frac{1}{\delta} \sum_{\pi^M \cap [t,t+\delta]} (X(t_{i+1}^M) - X(t_i^M))^2 \quad (16)$$

Note that in order to approximate the diffusion vector $(\sigma(X_{t_0}), \sigma(X_{t_1}), \dots, \sigma(X_{t_{N-1}}))$ one need to have observation of the underlying process X along a finer grid, i.e. $\sigma(X_{t_i})$ is calculated by talking sum square difference of L many observation of X between t_i and t_{i+1} . Once the σ vector has been identified, we can then construct the \mathbb{Q} -Brownian motion increment on any interval $[t, t + \delta]$, for $\delta > 0$,

$$B_{t+\delta}^{\mathbb{Q}} - B_t^{\mathbb{Q}} = \int_t^{t+\delta} \frac{dX_s}{\sigma(X_s)} \approx \frac{\sqrt{\delta}(X(t+\delta) - x(t))}{\sqrt{\sum_{\pi^M \cap [t,t+\delta]} (X(t_{i+1}^M) - X(t_i^M))^2}}. \quad (17)$$

leaning σ function from the vector $(\sigma(X_{t_0}), \sigma(X_{t_1}), \dots, \sigma(X_{t_{N-1}}))$ By considering the input-output pairs $\{(X_{t_i}, \sigma(X_{t_i}))\}$, we build a library $\Theta(X_{t_i})$ and rewrite (generalized) SINDy into a symbolic regression form as follows.

$$\Xi_{\sigma}^* = \arg \min_{\Xi_{\sigma}} \sum_{i=0}^{N-1} \|\sigma(X_{t_i}) - \Theta(X_{t_i})\Xi_{\sigma}\| + \|\Xi_{\sigma}\|_0, \quad (18)$$

where the first loss is to fit the model (i.e., the function σ), and the second term is referred to as sparsity regularization. This optimization problem can be solved using a sequential thresholding least-squares algorithm in SINDy. Since the coefficient of Ξ_{σ} is sparse, this optimization problem effectively identifies the symbolic functional form of the $\sigma(X_{t_i})$ (e.g., for the BS equation $\sigma(X_{t_i}) = \sigma X_{t_i}$). Note that from (16) we can not recover the terminal value $\sigma(X_{t_N})$, but once we estimate the σ function from (18) one can estimate $\sigma(X_{t_N})$, recovering the entire diffusion vector $(\sigma(X_{t_0}), \sigma(X_{t_1}), \dots, \sigma(X_{t_N}))$.

Step 2: constructing estimator for X_t via Stratonovich SDE. For the Itô SDE (13), the corresponding Stratonovich SDE has the following form,

$$\begin{aligned} X_t &= X_s + \int_s^t -\frac{1}{2}\sigma(X_u)\sigma'(X_u)du + \int_s^t \sigma(X_u) \circ dB_u^{\mathbb{Q}} \\ &:= X_s + \int_s^t A_0(X_u)du + \int_s^t \sigma(X_u) \circ dB_u^{\mathbb{Q}}, \end{aligned} \quad (19)$$

where we denote $A_0(X_t) = -\frac{1}{2}\sigma(X_t)\sigma'(X_t)$, which is commonly known as the Itô-Stratonovich correction term. For the Stratonovich SDE (19), applying the (Stratonovich) change of variable formula (i.e. $f(X_u) = f(X_s) + \int_s^u f'(X_r) \circ dX_r$) for the A_0 and σ functions around the initial point X_s , we get the following expansion. Under some nominal Hölder assumptions on the underlying process X , this approximation error is of order $|t|^{3/2}$ (i.e. $|t_{i+1} - t_i|^{\frac{3}{2}}$ on each time grid $[t_i, t_{i+1}]$).

$$\begin{aligned} X_t &= X_s + A_0(X_s) \int_s^t du + \int_s^t \int_s^u A'_0(X_r) \circ dX_r du + \sigma(X_s) \int_s^t \circ dB_u^{\mathbb{Q}} \\ &\quad + \int_s^t \int_s^u \sigma'(X_r) \circ dX_r \circ dB_u^{\mathbb{Q}}. \end{aligned}$$

Plugging the differential from of the dynamic (19) into the above expansion, applying the change of variable iteratively, and finally approximating $\sigma(X_u)$ for all $u \in [t_i, t_{i+1}]$ by $\sigma(X_{t_i})$ we get the following second-order expansion⁴ of the process X_t in the Stratonovich form,

$$\begin{aligned} X_t &= X_s + \psi_1^{s,t} \int_s^t du + \psi_2^{s,t} \int_s^t \circ dB_u + \psi_{12}^{s,t} \int_s^t \int_s^u dr \circ dB_u^{\mathbb{Q}} \\ &\quad + \psi_{21}^{s,t} \int_s^t \int_s^u \circ dB_r^{\mathbb{Q}} du + \psi_{22}^{s,t} \int_s^t \int_s^u \circ dB_r^{\mathbb{Q}} \circ dB_u^{\mathbb{Q}} \\ &\quad + \psi_{222}^{s,t} \int_s^t \int_s^u \int_s^r \circ dB_v^{\mathbb{Q}} \circ dB_r^{\mathbb{Q}} \circ dB_u^{\mathbb{Q}} + \varepsilon^{\Psi_2}, \end{aligned} \quad (20)$$

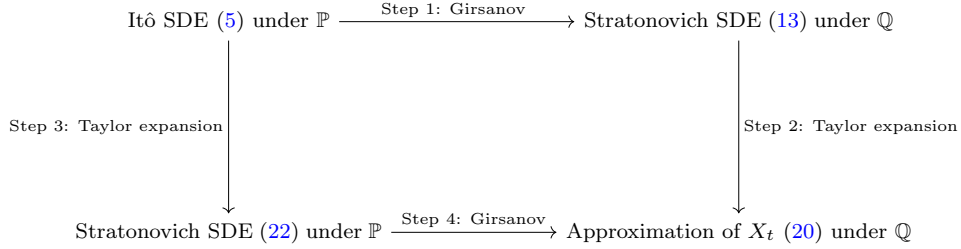
⁴by the second order we mean the error term is of the order $O(|t - s|^{2-\delta})$ for any $\delta > 0$.

where we denote ε^{Ψ_2} as the error for the higher-order Taylor expansion terms (see, e.g., [42]). The detailed derivation is provided in Appendix A. In the following, we will call the set $\Psi_2^{s,t}$ the second-order estimator of the diffusion process for the interval $[s, t]$, and denote it as

$$\Psi_2^{s,t} := \{\psi_1^{s,t}, \psi_2^{s,t}, \psi_{12}^{s,t}, \psi_{21}^{s,t}, \psi_{22}^{s,t}, \psi_{222}^{s,t}\}. \quad (21)$$

Note that the estimate of the set $\Psi_2^{s,t}$ does depend on the full data on the interval $[s, t]$, whereas theoretically the set $\Psi_2^{s,t}$ only depends on observations at time s . Essentially, the set $\Psi_2^{s,t}$ is a collection of different combinations of σ and all its derivatives evaluated at the initial value X_s . For example, $\psi_1^{s,t} = A_0(X_s)$ and $\psi_2^{s,t} = \sigma(X_s)$. Finally, we use the estimated \mathbb{Q} -Brownian motion $B^{\mathbb{Q}}$ from **Step 1** to find estimators in $\Psi_2^{s,t}$ for the second order model (20).

Next, instead of applying the Girsanov transformation first as done in **Step 1**, we will apply the Taylor expansion first directly for the Stratonovich SDE under Wiener measure \mathbb{P} in **Step 3**, and then apply the Girsanov transformation in the last step (**Step 4**) to construct the estimator of the function μ . The explicit algorithm is demonstrated in the following diagram.



Step 3: Taylor expansion of Stratonovich SDE under Wiener measure \mathbb{P} . Recall the Stratonovich SDE (8) with a (deterministic) starting time s (not necessarily 0) with respect to the physical measure \mathbb{P} :

$$X_t = X_s + \int_s^t \tilde{\mu}(X_u) du + \int_s^t \sigma(X_u) \circ dB_u^{\mathbb{P}}.$$

Applying stochastic Taylor expansion on $\tilde{\mu}$ and σ around the initial observation X_s , and truncating the Taylor expansion at level 2 (see e.g. [42]), we have the following (up to second order derivatives of $\tilde{\mu}$ and σ) Taylor expansion approximation of X_t under Wiener measure \mathbb{P} ,

$$\begin{aligned}
X_t = X_s &+ \tilde{\mu}(X_s) \int_s^t du + \sigma(X_s) \int_s^t \circ dB_u^{\mathbb{P}} \\
&+ \tilde{\mu}'(X_s) \tilde{\mu}(X_s) \int_s^t \int_s^u dr du + \tilde{\mu}'(X_s) \sigma(X_s) \int_s^t \int_s^u \circ dB_r^{\mathbb{P}} du \\
&+ \sigma'(X_s) \tilde{\mu}(X_s) \int_s^t \int_s^u dr \circ dB_u^{\mathbb{P}} + \sigma'(X_s) \sigma(X_s) \int_s^t \int_s^u \circ dB_r^{\mathbb{P}} \circ dB_u^{\mathbb{P}} \\
&+ ((\tilde{\mu}'(X_s))^2 \tilde{\mu}(X_s) + \tilde{\mu}''(X_s)(\tilde{\mu}(X_s))^2) \int_s^t \int_s^u \int_s^r dv dr du \\
&+ ((\tilde{\mu}'(X_s))^2 \sigma(X_s) + \tilde{\mu}''(X_s) \tilde{\mu}(X_s) \sigma(X_s)) \int_s^t \int_s^u \int_s^r \circ dB_v^{\mathbb{P}} dr du \\
&+ (\tilde{\mu}'(X_s) \sigma'(X_s) \tilde{\mu}(X_s) + \tilde{\mu}''(X_s) \tilde{\mu}(X_s) \sigma(X_s)) \int_s^t \int_s^u \int_s^r dv \circ dB_r^{\mathbb{P}} du \\
&+ (\tilde{\mu}'(X_s) \sigma'(X_s) \tilde{\mu}(X_s) + \sigma''(X_s)(\tilde{\mu}(X_s))^2) \int_s^t \int_s^u \int_s^r dv dr \circ dB_u^{\mathbb{P}} \\
&+ (\tilde{\mu}'(X_s) \sigma'(X_s) \sigma(X_s) + \tilde{\mu}''(X_s)(\sigma(X_s))^2) \int_s^t \int_s^u \int_s^r \circ dB_v^{\mathbb{P}} \circ dB_r^{\mathbb{P}} du \\
&+ (\tilde{\mu}'(X_s) \sigma'(X_s) \sigma(X_s) + \sigma''(X_s) \sigma(X_s) \tilde{\mu}(X_s)) \int_s^t \int_s^u \int_s^r \circ dB_v^{\mathbb{P}} dr \circ dB_u^{\mathbb{P}} \\
&+ ((\sigma'(X_s))^2 \tilde{\mu}(X_s) + \sigma''(X_s) \sigma(X_s) \tilde{\mu}(X_s)) \int_s^t \int_s^u \int_s^r dv \circ dB_r^{\mathbb{P}} \circ dB_u^{\mathbb{P}} \\
&+ ((\sigma'(X_s))^2 \sigma(X_s) + \sigma''(X_s)(\sigma(X_s))^2) \int_s^t \int_s^u \int_s^r \circ dB_v^{\mathbb{P}} \circ dB_r^{\mathbb{P}} \circ dB_u^{\mathbb{P}} + \varepsilon^{\tilde{\mu}, \sigma}, \quad (22)
\end{aligned}$$

where $\varepsilon^{\tilde{\mu}, \sigma}$ denotes the higher order approximation error term. The proof of this claim is postponed to the following Appendix A, along with the discussion of the error term $\varepsilon^{\tilde{\mu}, \sigma}$.

Step 4: Girsanov transformation. Applying the Girsanov theorem, substituting for all $r \in [s, t]$; $dB_r^{\mathbb{P}} = dB_r^{\mathbb{Q}} - \frac{\mu(X_r)}{\sigma(X_r)} dr$ into the Stratonovich SDE approximation (22), we have the following second order approximation expansion of X_t

$$\begin{aligned} X_t &= X_s - \frac{1}{2} \sigma(X_s) \sigma'(X_s) \int_s^t du + \sigma(X_s) \int_s^t \circ dB_u^{\mathbb{Q}} \\ &+ \left(\mu'(X_s) \sigma(X_s) - \mu(X_s) \sigma'(X_s) - \frac{1}{2} \sigma(X_s) \sigma'(X_s)^2 - \frac{1}{2} \sigma(X_s)^2 \sigma''(X_s) \right) \int_s^t \int_s^u \circ dB_r^{\mathbb{Q}} du \\ &- \frac{1}{2} \sigma(X_s) \sigma'(X_s)^2 \int_s^t \int_s^r du \circ dB_r^{\mathbb{Q}} + \sigma'(X_s) \sigma(X_s) \int_s^t \int_s^u \circ dB_r^{\mathbb{Q}} \circ dB_u^{\mathbb{Q}} \\ &+ ((\sigma'(X_s))^2 \sigma(X_s) + \sigma''(X_s) (\sigma(X_s))^2) \int_s^t \int_s^u \int_s^r \circ dB_v^{\mathbb{Q}} \circ dB_r^{\mathbb{Q}} \circ dB_u^{\mathbb{Q}} + \varepsilon^{\tilde{\mu}, \sigma} + \varepsilon^{\mu/\sigma}. \end{aligned} \quad (23)$$

where the error term $\varepsilon^{\tilde{\mu}, \sigma}$ is due to (22), and the error term $\varepsilon^{\mu/\sigma}$ is due to the approximation of $\frac{\mu(X_u)}{\sigma(X_u)}$ by the initial condition $\frac{\mu(X_s)}{\sigma(X_s)}$ for $u \in [s, t]$. We want to remark that only when $|t - s|$ is small the error term $\varepsilon^{\mu/\sigma}$ can be controlled and is of order $|t - s|^{2-\epsilon}$ for $|t - s|$ small and any $\epsilon > 0$, not for general s, t . In particular, following the Taylor expansion [5] and the Castell estimates [16], the error term $\varepsilon^{\tilde{\mu}, \sigma} + \varepsilon^{\mu/\sigma}$ follows a Gaussian tail estimate. The expected error (under $\mathbb{E}^{\mathbb{Q}}$) can be found in [46]. The proof of this claim is postponed to Appendix C.

Remark 3.1. As a consequence of the above approximation, we essentially restrict ourselves to the case when $\frac{\mu}{\sigma} \approx \text{constant}$ on each interval $[t_i, t_{i+1}]$. A higher-order Taylor approximation of $\frac{\mu(X_u)}{\sigma(X_u)}$ is also possible, which will relax the $\frac{\mu}{\sigma} \approx \text{constant}$ assumption; we leave it for future studies. We remark that by taking the proposed higher order Taylor expansion, the (24) will change accordingly.

Step 5: constructing estimator of μ . In this step we recursively calculate the drift vector $(\mu(X_{t_1}), \mu(X_{t_2}), \dots, \mu(X_{t_N}))$ under the assumption of know initial value $\mu(X_{t_0})$ is known. By comparing the coefficients of same iterated integrals of (20) from **Step 2** and (23) from **Step 4** on the interval $[t_0, t_1]$ and under the assumption of know initial value $\mu(X_{t_0})$ we calculate the drift $\mu(X_{t_1})$, than recursively calculate all the other drift terms. Under the assumption that σ is continuous, it is enough for short time uniqueness of ODE for the drift function μ in the interval $[t_i, t_{i+1}]$ for $|t_{i+1} - t_i| \ll 1$, and hence in the interval $[t_i, t_{i+1}]$ the drift function can be written as the (unique) solution of the following ODE with given initial value $\mu(x_{t_i})$ (which is estimated from the previous step)

$$\mu'(x) = a(x)\mu(x) + b(x), \quad (24)$$

where $a(x) = \frac{\sigma'(x)}{\sigma(x)}$ and $b(x) = \frac{2\psi_{21}^{[t_i, t_{i+1}]} + \sigma(x)\sigma'(x)^2 + \sigma(x)^2\sigma''(x)}{2\sigma(x)}$, and $\psi_{21}^{[t_i, t_{i+1}]}$ is defined in (20) from **Step 2** on the interal $[t_i, t_{i+1}]$. Note that we can identify the functional form of σ and its derivatives from **Step 1**. The proof is postponed to Appendix D.

Step 6: estimating the noise with \mathbb{P} -Brownian motion. By applying regression methods to find the estimator $\psi_{12}^{[t_i, t_{i+1}]}$ recursively using the model constructed from the martingale Brownian motion $B^{\mathbb{Q}}$. Applying **Step 1-5** to the single trajectory observation of the states $\{X_{t_i}\}_{i=1}^N$, we find the second order estimator for the drift vector μ at the time grid t_1, \dots, t_N as the solution of ODE (24). Then, applying the change of measure (14) to recover the noise increment vectors $(\Delta B_{t_0}^{\mathbb{P}}, \Delta B_{t_1}^{\mathbb{P}}, \dots, \Delta B_{t_{N-1}}^{\mathbb{P}})$ by using the following discretization scheme,

$$\Delta B_{t_i}^{\mathbb{Q}} = \Delta B_{t_i}^{\mathbb{P}} + \frac{\mu(X_{t_i})}{\sigma(X_{t_i})} \Delta t_i, \quad \text{for } i = 1, \dots, N, \quad (25)$$

where we use the convection $\Delta B_{t_i}^{\mathbb{P}} = B_{t_{i+1}}^{\mathbb{P}} - B_{t_i}^{\mathbb{P}}$ (similarly for $B^{\mathbb{Q}}$ and t).

Step 7: SSISDE to recover drift and diffusion function. We now present the *Stochastic Sparse Identification of Stochastic Differential Equation* (SSISDE) algorithm, which is able to precisely identify the form of the governing SDE (5)

$$dX_t = \mu(X_t)dt + \sigma(X_t)dB_t^{\mathbb{P}}.$$

If X_t and the noise $B_t^{\mathbb{P}}$ can be observed along the time grid $t_1 < \dots < t_N$, this can be viewed as a symbolic regression problem that

$$dX_t = \Theta_{\mu}(X_t) \Xi_{\mu} dt + \Theta_{\sigma}(X_t) \Xi_{\sigma} dB_t^{\mathbb{P}}, \quad (26)$$

which is motivated from the the *sparse identification of nonlinear dynamics* (SINDy) [14]. Following the idea of SINDy, According to **Step 6**, we have constructing the original noise increment $\{\Delta B_{t_i}^{\mathbb{P}}\}_{i=0}^{N-1}$ from observation data $\{X_{t_i}\}_{i=0}^N$. We construct symbolic regression for the following identity

$$\Delta X_{t_i} = \Theta_{\mu}(X_{t_i})\Xi_{\mu}\Delta t_i + \Theta_{\sigma}(X_{t_i})\Xi_{\sigma}\Delta B_{t_i}^{\mathbb{P}}, \quad (27)$$

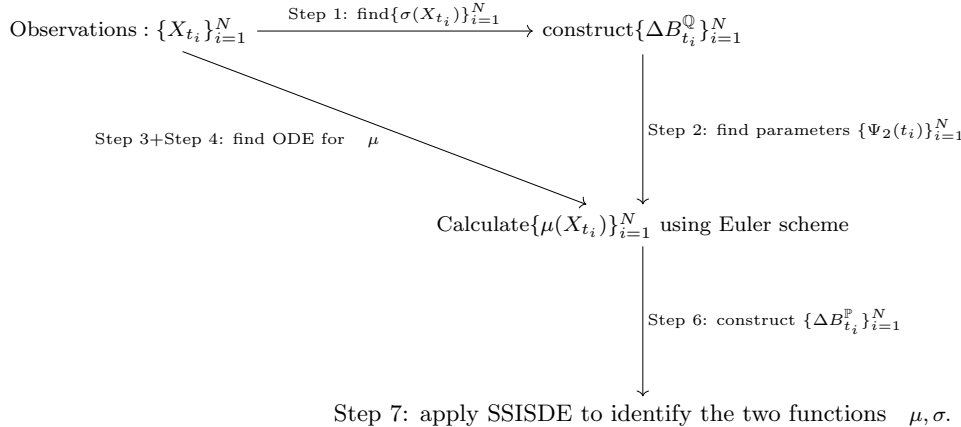
for $i = 0, \dots, N-1$. We denote Ξ_{σ} (and Ξ_{μ} respectively) as the unknown sparse matrix corresponding to function σ (and μ respectively). Similarly, we denote $\Theta_{\sigma}(\cdot)$ and $\Theta_{\mu}(\cdot)$ as the candidate models for σ and μ . We thus propose the following *Stochastic Sparse Identification of Stochastic Differential Equation* (SSISDE) algorithm, which can be written as a stochastic symbolic regression problem,

$$\arg \min_{\Xi_{\sigma}, \Xi_{\mu}} \sum_{i=0}^{N-1} \|\Delta X_{t_i} - \Theta_{\mu}(X_{t_i})\Xi_{\mu}\Delta t_i - \Theta_{\sigma}(X_{t_i})\Xi_{\sigma}\Delta B_{t_i}^{\mathbb{P}}\|_2^2 + \mathcal{R}_{\alpha, \rho}(\Xi_{\mu}, \Xi_{\sigma}), \quad (28)$$

where the first term is the residual L_2 -norm, and the second is a sparsity-inducing regularizer.

Remark 3.2. The Stochastic Sparse Identification of Stochastic Differential Equation (SSISDE) (28) only takes input data ΔX_{t_i} and the estimated noise $\Delta B_{t_i}^{\mathbb{P}}$, which is different from the SINDy form (18) in **Step 5**. In the end, one can compare the estimated symbolic forms for the function σ . In general, we only use (18) in **Step 5** to construct the estimate of the drift vector $\mu(X_{t_i})$ and the desired noise $\Delta B_{t_i}^{\mathbb{P}}$.

The main algorithm is described below.



4 Numerical Experiments

4.1 Model description

In this section, we demonstrate the performance of our method for estimating the drift, diffusion function, and noise vector across several numerical examples. We assume the process X_t satisfies the dynamics as given in Eq. (5). We simulate sample paths using a standard time-discretization scheme, such as the Euler-Maruyama scheme. With access to the data, we approximate its quadratic variation $[X]_{\pi, t_i}$ for each time index $t_i : 0 \leq i \leq n$ where $t_0 = 0, t_n = T$, $n = 100000$, and $T = 1$ of a chosen uniform partition π . The quadratic variation satisfies the ordinary differential equation $d[X]_{\pi, t} = (\sigma(X_t))^2 dt$. On estimated $Y_t = [X]_{\pi, t}$, we solve the symbolic regression problem (18) to get the functional form of $(\sigma(X_t))^2$ and hence $\sigma(X_t)$. The L_0 penalty $\|\Xi_{\sigma}\|_0$ in Eq. (18) induces sparsity, but since we focus only on estimating $\sigma(X_t)$ accurately, no regularization coefficient is included. We know that under risk-neutral probability \mathbb{Q} , the dynamics of X_t satisfy $dX_t = \sigma(X_t)dB_t^{\mathbb{Q}}$, which can be used to get the $B_t^{\mathbb{Q}}$ vector assuming it starts at zero. Now we have access to the primary process $(t_i, B_{t_i}^{\mathbb{Q}})$ for $0 \leq i \leq N$. We extend the features by using the idea of the iterated Stratonovich integral of the primary process up to order $|t-s|^{2-\epsilon}$, for any $\epsilon > 0$, i.e., the integrals corresponding to the following coefficients

$$\Psi_2 := \{\psi_1, \psi_2, \psi_{12}, \psi_{21}, \psi_{22}, \psi_{222}\}.$$

We choose a sub-partition $\{j_k\}_{k=0}^M, M \ll N$ of the partition π such that $t_{j_0} = t_0, t_{j_M} = t_N$ with $M = 1000$. On each sub-interval $[t_{j_k}, t_{j_{k+1}}]$ of this sub-partition, X is regressed against above features to estimate the values of coefficients in the Ψ_2 at $t = t_{j_k}$ for $k = 0, \dots, M$. We would also like to remark that using (36) one can estimate Ψ_2 using the symbolic form of σ recovered in **Step-1**, without using the regression method used in the classical signature model.

The ODE (24) is then solved to get the vector of $\mu(X_{t_{j_k}})$ for each t_{j_k} . Furthermore, we use the discretization scheme (25) to predict the noise increment vectors $(\Delta B_{t_{j_0}}^{\mathbb{P}}, \Delta B_{t_{j_1}}^{\mathbb{P}}, \dots, \Delta B_{t_{j_M}}^{\mathbb{P}})$ hence the noise $B^{\mathbb{P}}$ by assuming it starts at zero. Finally, we use the *SSISIDE* (28) to recover the symbolic form of drift $\mu(X_t)$ and diffusion $\sigma(X_t)$. We describe the model-selection procedure, i.e., k -fold time-series cross-validation, the CV error δ , and the choice of the optimal sparsity level, before presenting the numerical examples.

4.1.1 Model selection via k -fold time-series cross-validation

We adopt an elastic-net penalty [37] in the penalized identification problem (28), namely

$$\mathcal{R}_{\alpha, \rho}(\Xi_{\mu}, \Xi_{\sigma}) = \alpha \left(\rho \|\beta\|_1 + \frac{1-\rho}{2} \|\beta\|_2^2 \right), \quad \beta := \begin{bmatrix} \Xi_{\mu} \\ \Xi_{\sigma} \end{bmatrix},$$

with $\|\cdot\|_1$ and $\|\cdot\|_2$ the usual vector norms. The penalty strength $\alpha > 0$ and mixing parameter $\rho \in [0, 1]$ are hyperparameters that control sparsity and shrinkage in $(\Xi_{\mu}, \Xi_{\sigma})$ ($\rho = 1$ recovers Lasso; $\rho = 0$ Ridge). We select (α, ρ) by k -fold *time-series* cross-validation [60] (no shuffling across time): let $\{A_j\}_{j=1}^k$ partition the index set $\{1, \dots, N-1\}$ into k contiguous, non-overlapping validation blocks, and define $B_j := \bigcup_{\ell \neq j} A_{\ell}$ as the complementary training indices. For each candidate pair (α, ρ) and each fold j , we fit (28) on B_j to obtain $(\widehat{\Xi}_{\mu}^{(j)}, \widehat{\Xi}_{\sigma}^{(j)})$, and compute the mean squared one-step prediction error on A_j :

$$\delta_j^2(\alpha, \rho) := \frac{1}{|A_j|} \sum_{i \in A_j} \left\| \Delta X_{t_i} - \Theta_{\mu}(X_{t_i}) \widehat{\Xi}_{\mu}^{(j)} \Delta t_i - \Theta_{\sigma}(X_{t_i}) \widehat{\Xi}_{\sigma}^{(j)} \Delta B_{t_i}^{\mathbb{P}} \right\|_2^2.$$

The k -fold CV score and its standard error are

$$\bar{\delta}(\alpha, \rho) = \frac{1}{k} \sum_{j=1}^k \delta_j(\alpha, \rho), \quad \text{SE}(\alpha, \rho) = \sqrt{\frac{1}{k(k-1)} \sum_{j=1}^k (\delta_j(\alpha, \rho) - \bar{\delta}(\alpha, \rho))^2}.$$

We evaluate $\bar{\delta}$ on a logarithmic grid $\alpha \in \Lambda$ and a discrete set $\rho \in \mathcal{P}$ (including $\rho = 1$ for Lasso). To reduce shrinkage bias, after solving (28) on each training fold we refit an ordinary least-squares model *restricted to the active set* (nonzero entries of $(\widehat{\Xi}_{\mu}^{(j)}, \widehat{\Xi}_{\sigma}^{(j)})$) before scoring on A_j .⁵

4.1.2 Choice of the final model

Let $(\alpha_*, \rho_*) = \arg \min_{\alpha, \rho} \bar{\delta}(\alpha, \rho)$ and define the one-standard-error [37] threshold

$$\varepsilon = \bar{\delta}(\alpha_*, \rho_*) + \text{SE}(\alpha_*, \rho_*).$$

Among all (α, ρ) with $\bar{\delta}(\alpha, \rho) \leq \varepsilon$, we pick the *simplest* model, i.e., the one with the smallest support size (fewest nonzeros in $(\Xi_{\mu}, \Xi_{\sigma})$); ties are broken toward larger α (and larger ρ when applicable). This yields $(\alpha^{\dagger}, \rho^{\dagger})$ and the corresponding $(\widehat{\Xi}_{\mu}, \widehat{\Xi}_{\sigma})$. We then refit (28) on the *full* dataset with $(\alpha^{\dagger}, \rho^{\dagger})$, followed by the same restricted least-squares de-biasing on the selected support, and we report the in-sample mean squared error as a summary of fit quality.

4.1.3 Optimally sparse size

It is often informative to summarize CV results as a function of the active-set sizes

$$n_{\mu} := \|\widehat{\Xi}_{\mu}\|_0, \quad n_{\sigma} := \|\widehat{\Xi}_{\sigma}\|_0,$$

where $\|\cdot\|_0$ counts nonzero entries [see e.g. [25], [13]]. Grouping all grid points (α, ρ) that yield the same $n \in \mathbb{N}$, define

$$\delta(n) = \min_{(\alpha, \rho): \|\widehat{\Xi}\|_0 = n} \bar{\delta}(\alpha, \rho), \quad \widehat{\Xi} := (\widehat{\Xi}_{\mu}, \widehat{\Xi}_{\sigma}).$$

Empirically, $\delta(n)$ typically exhibits three regimes: (i) underfitting at very small n (large error), (ii) a flat “good” region where accuracy is stable across several n , and (iii) overfitting at very large n (rising error). We define the *optimally sparse* sizes $\tilde{n}_{\mu}, \tilde{n}_{\sigma}$ as the smallest n whose error lies within one standard error of the minimum of $\delta(n)$ (a size-based analogue of the 1-SE rule). We compare them with the sizes actually selected by $(\alpha^{\dagger}, \rho^{\dagger})$. For completeness we also provide “ δ vs. n ” plots with ± 1 SE bands for both μ and σ .

⁵All feature normalizations are computed *using training data of each fold only* and then applied to both training and validation rows to prevent temporal leakage.

4.1.4 Practical settings used in our experiments

Unless stated otherwise, we use $k = 7$ contiguous folds, a logarithmic grid $\Lambda = \{\alpha_{\min}, \dots, \alpha_{\max}\}$ spanning several decades for α , and $\mathcal{P} = \{0.3, 0.4, 0.5, 0.7, 0.85, 0.95, 1.0\}$ for ρ (with $\rho = 1.0$ recovering Lasso). Feature blocks are built as

$$\Theta_\mu(X_{t_i}) \Delta t_i \quad \text{and} \quad \Theta_\sigma(X_{t_i}) \Delta B_{t_i}^{\mathbb{P}},$$

with RMS column normalization applied separately to each block on the training portion of each fold. All reported coefficients are de-biased by restricted least squares on the selected support. Alongside $(\alpha^\dagger, \rho^\dagger)$ and $(\tilde{n}_\mu, \tilde{n}_\sigma)$, we provide the final model size, validation curves/surfaces, and δ vs. n summaries to document the sparsity-accuracy trade-off achieved by (28) in each example.

4.1.5 Methods of estimating ψ_{21} and hence $\mu(X_t)$

Here we present two methods to estimate the parameter ψ_{21} from (20). The estimation of ψ_{21} will lead to estimating $\mu(X_t)$ using 44.

Method 1: To begin with, we approximate ψ_{21} by regressing X_t against the iterated integrals in (20) for each $t \in [t_{j_k}, t_{j_k+1})$. The coefficient of $\int_{t_{j_k}}^{t_{j_k+1}} \int_s^u \sigma dB_r^{\mathbb{Q}} du$ is then extracted to get an estimate of ψ_{21} on each interval. This procedure is repeated for $k : k = 0, \dots, M - 1$.

Method 2: Secondly, to avoid the regression error from fitting X_t against the iterated integral terms, we use the closed-form coefficient of $\int_s^t \int_s^u \sigma dB_r^{\mathbb{Q}} du$ from Eq.(36) to compute ψ_{21} . Since the coefficient only depends on $\sigma(X_t)$, no additional data fitting is required. We simply use the value of $\sigma(X_t)$ and its first two derivatives at $t = t_k$ for $k = 0, \dots, M - 1$ to recover ψ_{21} on each sub-interval $[t_{j_k}, t_{j_k+1})$.

Once ψ_{21} is recovered, we compute $b(X_{t_k}) = \frac{2\psi_{21}^{t_k, t_{k+1}} + \sigma(X_{t_k})\sigma'(X_{t_k})^2 + \sigma(X_{t_k})^2\sigma''(X_{t_k})}{2\sigma(X_{t_k})}$ and substitute this value into the Euler scheme 44 to estimate $\mu(X_{t_k})$ for $k = 0, \dots, M - 1$.

Finally, let us present and discuss the results of our numerical experiments in the case of different classical examples.

4.2 Time-shifted Brownian motion

Consider the SDE

$$dX_t = \mu dt + \sigma dB_t^{\mathbb{P}}, \quad (29)$$

where $\mu > 0$ and $\sigma > 0$ are constants. This SDE does not satisfy the ergodicity assumption. The choice of this particular SDE is motivated from the earliest model of stock price path first introduced by Bachelier in his thesis [7]. The drift and diffusion coefficients are taken to be constant, with $\mu = 0.5$ and $\sigma = 1.0$ in our experiments. The explicit solution of the stochastic differential equation is given by $X_t = X_0 + \mu t + \sigma B_t^{\mathbb{P}}$.

The solution X_t to Eq. (29) was simulated using Euler-Maruyama scheme. It could also be achieved by using the exact solution of the SDE. Before using the penalized residual (28) to identify the drift and diffusion function, the diffusion function was approximated, and the risk-neutral Brownian motion $B_{t_i}^{\mathbb{Q}}$ was estimated for $0 \leq i \leq N$. We then approximated the drift $\mu(X_t)$ using Method 1 and Method 2, as described in Subsection 4.1.5. The corresponding results are reported in Figure 1.

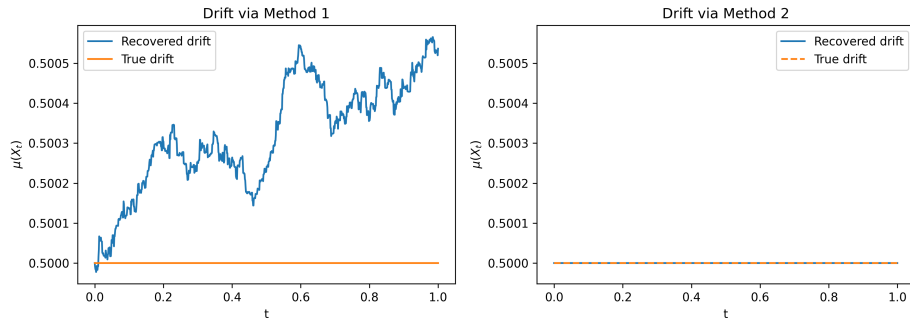


Figure 1: The true and the predicted drift $\mu(X_t)$ using Method 1 and Method 2. Little deviation of the approximate value of $\mu(X_t)$ in the Left figure from its true value is due to error in approximating ψ_{21} via regression. On the other hand, the approximate value of $\mu(X_t)$ in right figure exactly overlaps the true value of $\mu(X_t)$.

We now look at how the choice of the quantity ψ_{21} affects the recovery of the drift, diffusion function, and noise from a single path trajectory. In both cases we work with the same penalized residual (28) and use polynomial libraries

$$\Theta_\mu(x) = \{1, x, \dots, x^5\}, \quad \Theta_\sigma(x) = \{1, x, \dots, x^5\}.$$

The regularization parameters (α, ρ) are chosen by k -fold time-series cross-validation with $k = 7$. We search over a logarithmic grid for α and a small discrete set of ρ , then de-bias on the selected support and apply the 1-SE rule to prefer simpler models.

Case 1: Here in the first experiment we use [Method 1](#) to approximate the value of ψ_{21} . The cross-validation surface and curves (Fig. 2) show a wide region where the validation error is almost flat, and the chosen point $(\alpha^\dagger, \rho^\dagger)$ lies inside this near-optimal plateau and is $(\alpha^\dagger, \rho^\dagger) \approx (7.36 \times 10^{-5}, 0.70)$. The δ -versus- n summaries in Fig. 3 select $n_\mu = 1$ and $n_\sigma = 1$, so each block keeps only one non-zero term; adding more terms does not improve the error in any visible way. At these hyperparameters, the recovered drift and diffusion functions are

$$\hat{\mu}(x) = 0.000265 x + 0.499733, \quad \hat{\sigma}(x) = 1.0002.$$

They stay very close to the true constant values (see Fig. 4(a)–(b)), although the recovered drift shows some small fluctuations in time. In spite of this the recorded MSE was too small i.e., $\text{MSE} = 6.959 \times 10^{-16}$. The reconstructed noise process tracks the driving Brownian motion quite well, and the path simulated under the learned model is practically indistinguishable from the observed trajectory (Fig. 4(c)–(d)). This suggests that the method can capture the main dynamics even when ψ_{21} is only approximated.

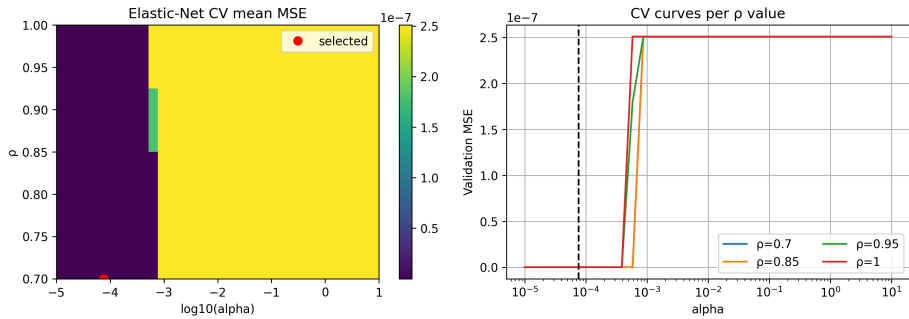


Figure 2: Time-series CV over (α, ρ) with de-biasing on the active set; the selected point $(\alpha^\dagger, \rho^\dagger) = (7.36 \times 10^{-5}, 0.70)$ lies on a broad near-optimal basin.

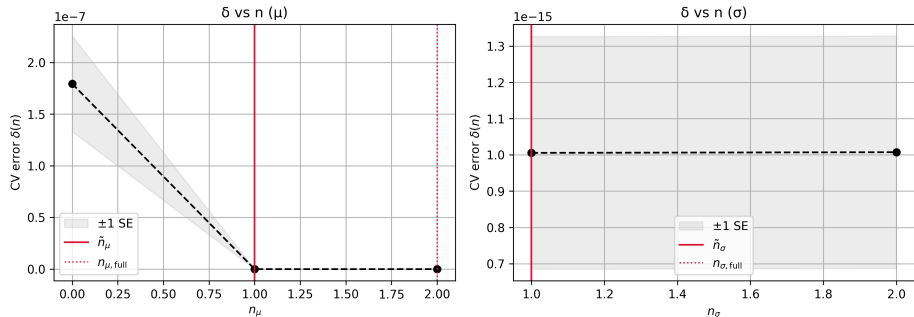


Figure 3: Validation error $\delta(n)$ vs. support size n with ± 1 SE bands for the drift and diffusion blocks. The vertical markers indicate the optimally sparse sizes and the sizes of the final full-data models.

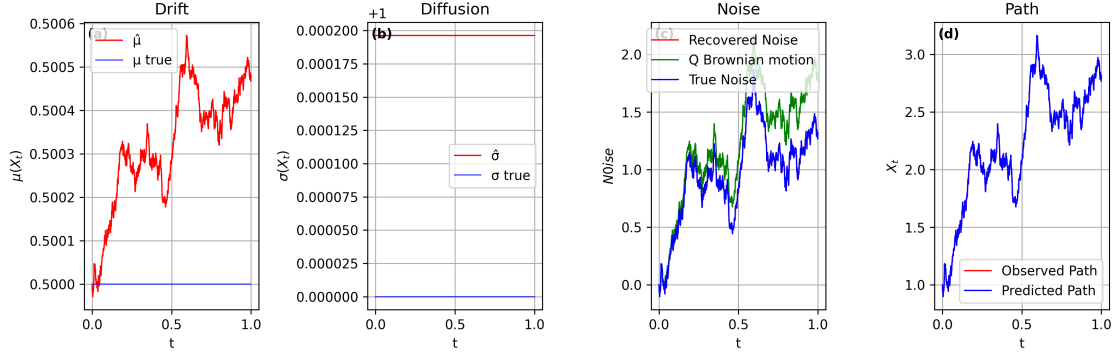


Figure 4: (a) The true $\mu(X_t)$ and reconstructed $\hat{\mu}(X_t)$ and (b) The true $\sigma(X_t)$ and reconstructed $\hat{\sigma}(X_t)$ are plotted against time on the interval $[0, 1]$. (c) The true noise, i.e., Brownian motion B^P that was used to simulate the actual path, the recovered noise, and the \mathbb{Q} -Brownian motion are plotted against time. (d) The actual path of the data X_t and the reconstructed one from the $\hat{\mu}(X_t)$ and $\hat{\sigma}(X_t)$ are plotted against time. Each vector is of length M with $M = 1000$.

Case 2: In the second experiment, we repeat exactly the same procedure, but now we use the value of ψ_{21} computed by using [Method 2](#). The cross-validation plots in Fig. 5 again display a broad flat region of low validation error, and the selected $(\alpha^\dagger, \rho^\dagger) = (5.82 \times 10^{-4}, 0.85)$ is very much close to the one in the first case. The corresponding δ -versus- n curves in Fig. 6 once more pick $n_\mu = 1$ and $n_\sigma = 1$.

With this more accurate value of ψ_{21} , the recovered drift and diffusion along the path are almost perfectly flat and lie on top of the true coefficients (Fig. 7(a)–(b)). The recovered drift and diffusion functions are

$$\hat{\mu}(x) = 0.5, \quad \hat{\sigma}(x) = 1.0002,$$

with very small $\text{MSE} = 3.497 \times 10^{-31}$. The reconstructed noise now overlaps the driving noise very closely, and the simulated path matches the data path almost exactly (Fig. 7(c)–(d)). Compared with the regression case, using the exact ψ_{21} mainly smooths out the estimated coefficients; the overall picture of the dynamics remains the same.

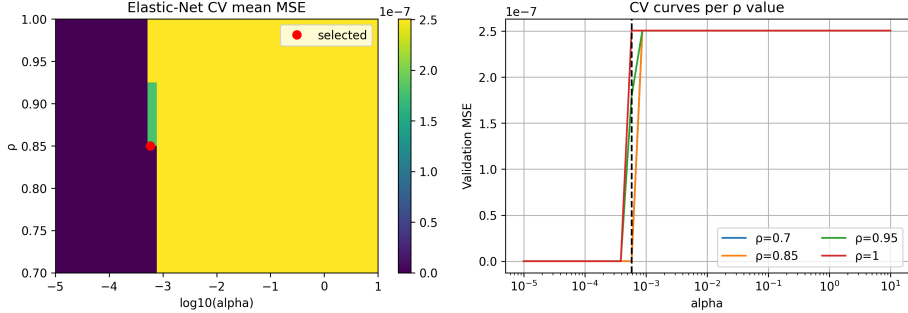


Figure 5: Time-series CV over (α, ρ) with de-biasing on the active set; the selected point $(\alpha^\dagger, \rho^\dagger) = (5.82 \times 10^{-4}, 0.85)$ lies on a broad near-optimal basin.

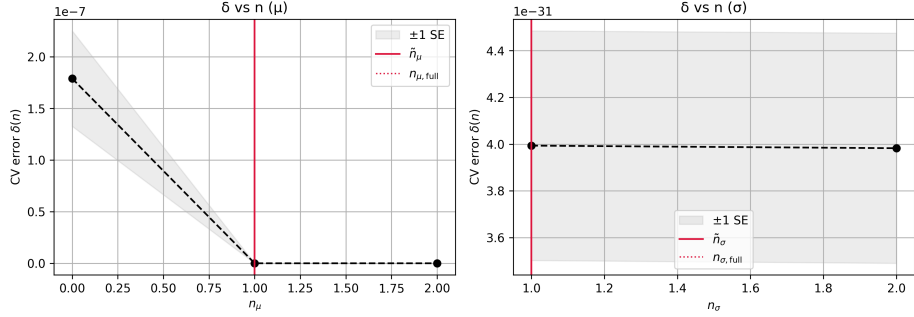


Figure 6: Validation error $\delta(n)$ vs. support size n with ± 1 SE bands for the drift and diffusion blocks. The vertical markers indicate the optimally sparse sizes and the sizes of the final full-data models.

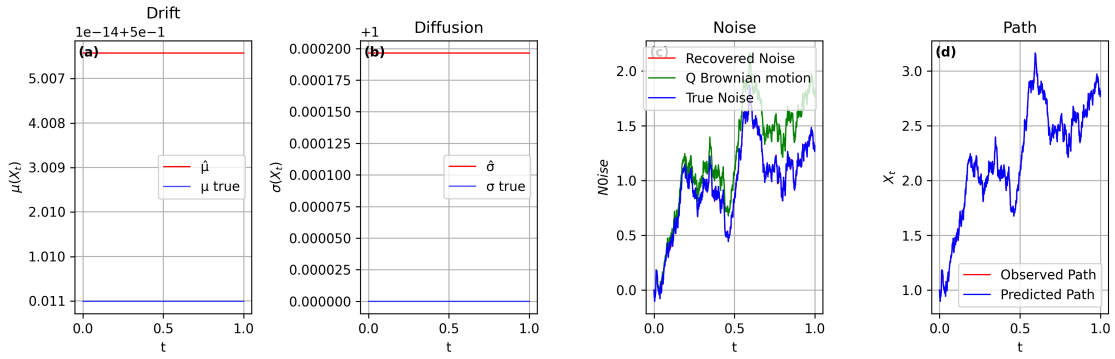


Figure 7: (a) The true $\mu(X_t)$ and reconstructed $\hat{\mu}(X_t)$ and (b) The true $\sigma(X_t)$ and reconstructed $\hat{\sigma}(X_t)$ are plotted against time on the interval $[0, 1]$. (c) The true noise, i.e., Brownian motion $B^{\mathbb{P}}$ that was used to simulate the actual path, the recovered noise, and the \mathbb{Q} -Brownian motion are plotted against time. (d) The actual path of the data X_t and the reconstructed one from the $\hat{\mu}(X_t)$ and $\hat{\sigma}(X_t)$ are plotted against time. Each vector is of length M with $M = 1000$.

4.3 Black–Scholes model

Consider the Black–Scholes SDE

$$dX_t = \mu X_t dt + \sigma X_t dB_t^{\mathbb{P}}, \quad (30)$$

where μ and $\sigma > 0$ are two constants, and the solution is a Geometric Brownian motion. This is an example of an SDE that does not satisfy the ergodicity assumption. It is the widely used dynamics for stock prices in finance. The idea traces back to Osborne and Samuelson's lognormal price hypothesis [53] and was formalized in the Black–Scholes–Merton framework [11] as geometric Brownian motion. The drift term is linear in the price, μX_t , and shows a proportional (percentage) expected rate of return. The diffusion term is also linear, $\sigma X_t dB_t^{\mathbb{P}}$, and σ is taken positive because it represents standard deviation, and any negative sign can be absorbed by flipping the Brownian motion. In short, the drift part governs the systematic trend while the diffusion part quantifies how volatile the price is around that trend.

The path X_t solving the Black–Scholes SDE (30) was simulated using the Euler–Maruyama scheme by taking $\mu = 0.5$ and $\sigma = 0.3$. Similar to the previous example, before applying the penalized residual (28) to recover the drift and diffusion, we first approximated the diffusion term and estimated the risk-neutral Brownian motion $B_{t_i}^{\mathbb{Q}}$ for $0 \leq i \leq N$. We then estimated the drift $\mu(X_t)$ using the two choices of ψ_{21} provided by [Method 1](#) and [Method 2](#) (see Subsection 4.1.5). The resulting drift estimates are shown in Figure 8.

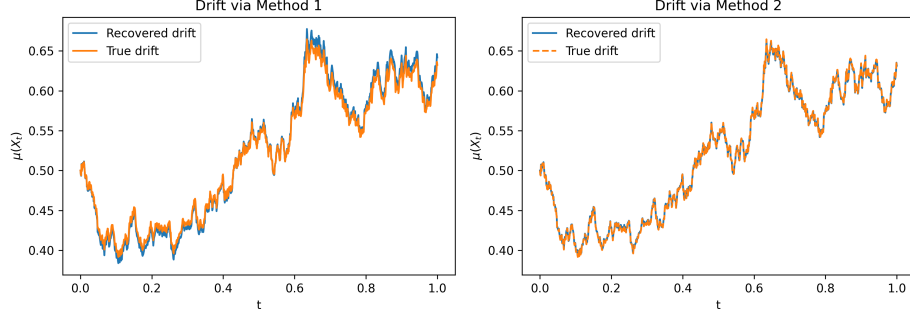


Figure 8: Comparison of the true drift $\mu(X_t)$ with its reconstructions using two approximations of ψ_{21} : (Left) ψ_{21} obtained via [Method 1](#); (Right) ψ_{21} computed using [Method 2](#). The small discrepancy in the **Left** panel is attributed to regression error in ψ_{21} . In the **Right** panel, the recovered drift overlaps the true drift.

We now examine how the choice of ψ_{21} influences the recovery of the drift, diffusion, and noise from a single observed path. In both settings, we use the same penalized residual (28) and the same polynomial libraries,

$$\Theta_\mu(x) = \{1, x, \dots, x^5\}, \quad \Theta_\sigma(x) = \{1, x, \dots, x^5\}.$$

The parameters (α, ρ) are selected using k -fold time-series cross-validation with $k = 7$. We scan a logarithmic grid for α and a small discrete set for ρ . After selecting the active terms, we re-estimate the coefficients by restricted least squares to reduce bias. Finally, we use the 1-SE rule to favor a simpler model when its performance is close to the best one.

Case 1: In the first experiment, we use the value of ψ_{21} obtained by applying [Method 1](#). The cross-validation heatmap and the CV curves in Fig. 9 indicate a broad region where the validation error changes very little. The selected pair $(\alpha^\dagger, \rho^\dagger)$ lies inside this stable region and is approximately

$$(\alpha^\dagger, \rho^\dagger) \approx (3.87 \times 10^{-4}, 0.85).$$

The δ -versus- n plots in Fig. 10 suggest $n_\mu = 1$ and $n_\sigma = 2$. This means the drift block keeps a single active term, while the diffusion block keeps two terms; adding more terms does not lead to a visible improvement in the validation error. With these hyperparameters, the recovered functions take the form

$$\hat{\mu}(x) = 0.503773 x, \quad \hat{\sigma}(x) = 0.00323797 + 0.295761 x.$$

These estimates are close to the expected linear structure of the model, and the reconstructions of $\mu(X_t)$ and $\sigma(X_t)$ track the true curves well; see Fig. 11(a)–(b). The overall fit is strong, with a small mean squared error $\text{MSE} = 5.244 \times 10^{-9}$. The recovered noise follows the driving signal closely, and the path generated using $\hat{\mu}$ and $\hat{\sigma}$ is almost indistinguishable from the observed trajectory; see Fig. 11(c)–(d). Overall, these results indicate that the method can still recover the main dynamics when ψ_{21} is obtained via regression.

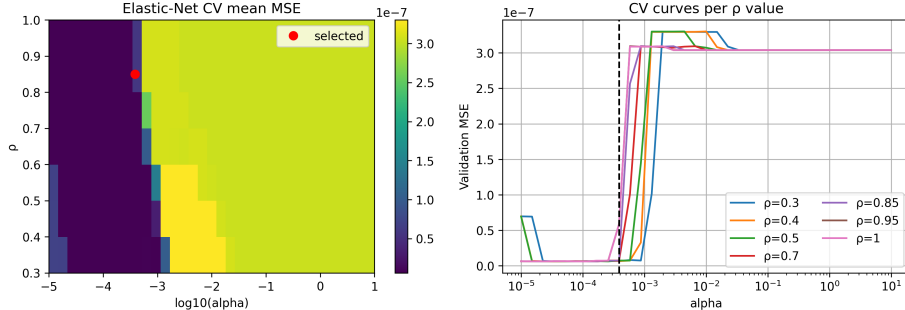


Figure 9: Time-series CV over (α, ρ) with de-biasing on the active set. The selected point $(\alpha^\dagger, \rho^\dagger) \approx (3.87 \times 10^{-4}, 0.85)$ lies in a broad near-optimal region.

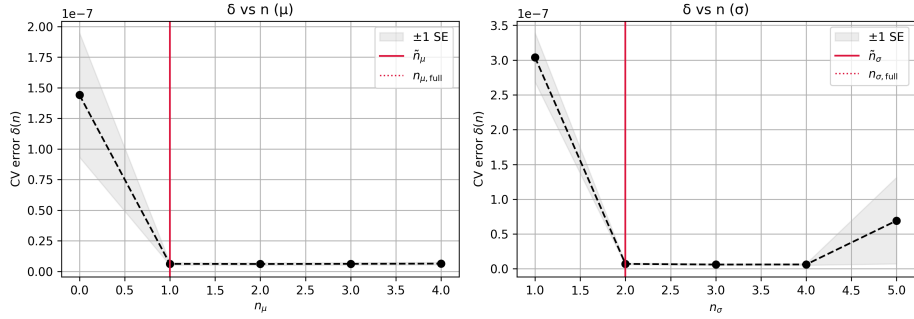


Figure 10: Validation error $\delta(n)$ versus support size n with ± 1 SE bands for the drift and diffusion blocks. The selected sizes are $n_\mu = 1$ and $n_\sigma = 2$, indicating sparse yet stable models.

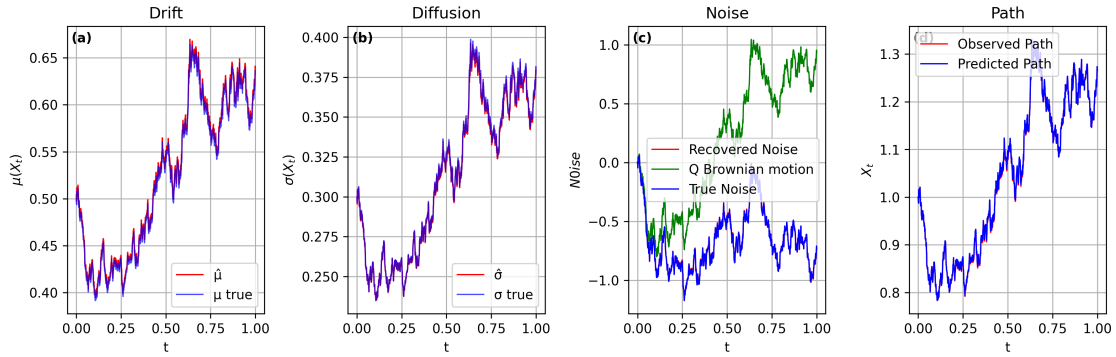


Figure 11: (a) True $\mu(X_t)$ and reconstructed $\hat{\mu}(X_t)$. (b) True $\sigma(X_t)$ and reconstructed $\hat{\sigma}(X_t)$. (c) True noise, recovered noise, and the \mathbb{Q} -Brownian motion. (d) Observed path X_t and the path simulated using the recovered $\hat{\mu}(X_t)$ and $\hat{\sigma}(X_t)$. Each vector is of length M with $M = 1000$.

Case 2: In the second experiment, we follow the same steps as in the first one, but now we use the value of ψ_{21} computed using [Method 2](#). The cross–validation heatmap and CV curves in Fig. 12 again show a wide region where the validation error is almost unchanged. The selected hyperparameters lie inside this stable region and are

$$(\alpha^\dagger, \rho^\dagger) \approx (3.87 \times 10^{-4}, 0.85),$$

which is very close to the choice obtained when ψ_{21} is estimated by regression. The δ -versus- n summaries in Fig. 13 select $n_\mu = 1$ and $n_\sigma = 2$, so the learned model remains sparse; adding more terms does not visibly reduce the CV error.

With this analytic ψ_{21} , the recovered drift and diffusion are

$$\hat{\mu}(x) = 0.501688 x, \quad \hat{\sigma}(x) = 0.00318241 + 0.295818 x,$$

with a small mean squared error $\text{MSE} = 5.192 \times 10^{-9}$. Along the observed trajectory, the reconstructed $\mu(X_t)$ and $\sigma(X_t)$ track the true curves closely (Fig. 14(a)–(b)). The recovered noise also follows the driving signal well, and the simulated path under the learned model nearly overlaps the observed path (Fig. 14(c)–(d)). Overall, using the analytic ψ_{21} mainly refines the estimates slightly, while the main dynamics remain consistent with the regression-based case.

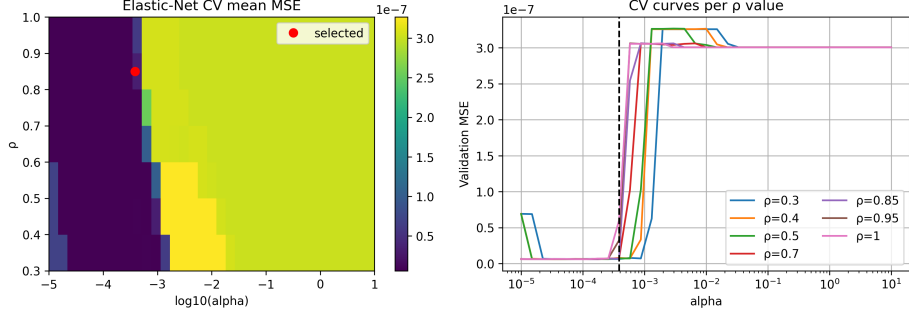


Figure 12: Time-series CV over (α, ρ) with de-biasing on the active set. The selected point $(\alpha^\dagger, \rho^\dagger) \approx (3.87 \times 10^{-4}, 0.85)$ lies in a broad near-optimal region.

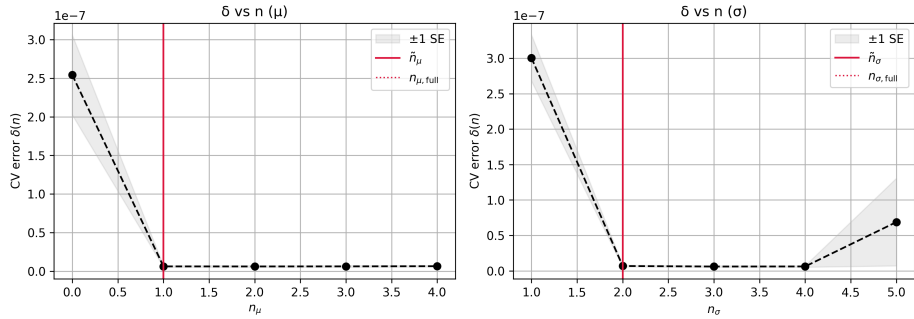


Figure 13: Validation error $\delta(n)$ versus support size n with ± 1 SE bands for the drift and diffusion blocks. The selected sparse sizes are $n_\mu = 1$ and $n_\sigma = 2$.

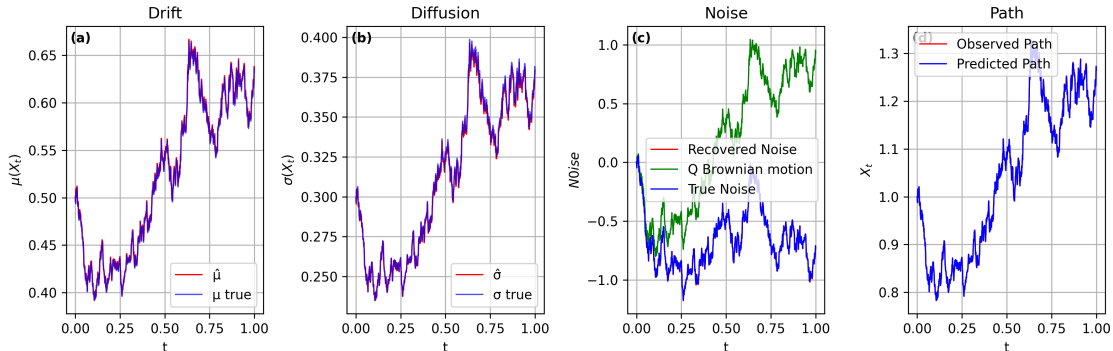


Figure 14: (a) True and recovered drift $\mu(X_t)$. (b) True and recovered diffusion $\sigma(X_t)$. (c) True noise, recovered noise, and the \mathbb{Q} -Brownian motion. (d) Observed and reconstructed paths of X_t . Each vector has length $M = 1000$.

4.4 Quadratic coefficients SDE

In this example, we study the SDE with quadratic drift and diffusion,

$$dX_t = \underbrace{(0.7 X_t + 0.3 X_t^2)}_{\mu(X_t)} dt + \underbrace{(0.5 X_t + 0.1 X_t^2)}_{\sigma(X_t)} dB_t^{\mathbb{P}}, \quad (31)$$

which belongs to the broader class of polynomial/CEV-type diffusions [23]. Unlike geometric Brownian motion, (31) features state-dependent nonlinearities in *both* the drift and the diffusion.

Because (31) has quadratic drift and diffusion with positive coefficients, the model may in principle exhibit explosive behavior over long time intervals. Since our goal is identification on the finite interval $[0, 1]$, we adopt

a simple safeguard in the simulation step to ensure that the generated trajectory remains finite i.e., we impose large absorbing bounds $[-L, L]$ such that $-L < X_0 < L$. Specifically, if the simulated path X_t ever hits either boundary $\pm L$, we set $X_t = 0$ for the remainder of the time interval. This truncation acts only as a numerical protection against rare large deviations that could otherwise dominate the regression and produce unstable estimates. In our experiments, the trajectory does not reach $\pm L$, indicating that the simulated sample is non-explosive on $[0, 1]$ and that the reported identification results reflect the genuine dynamics of (31) over the observation interval $[0, 1]$.

In line with the previous examples, we illustrate the full identification pipeline on this one-dimensional SDE and recover both the drift and diffusion function from a single trajectory via the penalized residual (28). The feature libraries for drift and diffusion are polynomial dictionaries

$$\Theta_\mu(x) = \{1, x, x^2, x^3, x^4, x^5\}, \quad \Theta_\sigma(x) = \{1, x, x^2, x^3, x^4, x^5\},$$

so that the analytic basis functions used to generate the data are the first two non-constant monomials $[x, x^2]$ in each dictionary. Hyperparameters (α, ρ) are selected by k -fold time-series cross-validation with $k = 7$, using a logarithmic grid $\alpha \in \{\text{geomspace}(10^{-5}, 10^1, 35)\}$ and $\rho \in \{0.3, 0.4, 0.5, 0.7, 0.85, 0.95, 1.0\}$. After each penalized fit on the training folds, we de-bias by restricted least squares on the active support before scoring on the validation fold, and apply the 1-SE rule to favor parsimony.

Following the same procedure as before, we approximate the diffusion vector and recover the \mathbb{Q} -Brownian motion $B^\mathbb{Q}$. Next, we recover $\mu(X_t)$ by plugging in ψ_{21} computed via [Method 1](#) and [Method 2](#) (see Subsection 4.1.5). Figure 15 compares the two drift estimates.

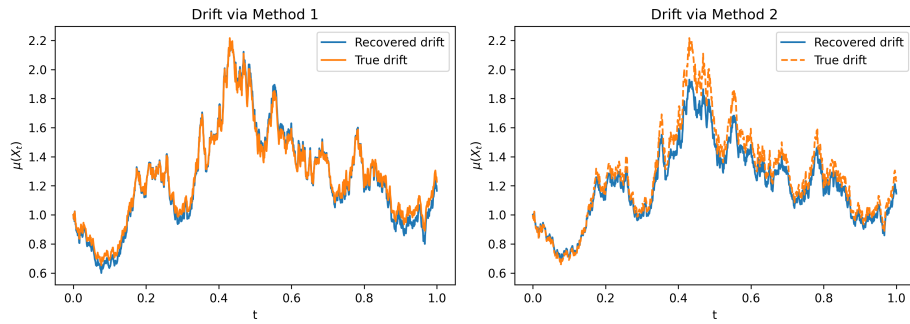


Figure 15: Comparison of the true drift $\mu(X_t)$ with its reconstructions using two approximations of ψ_{21} : (Left) ψ_{21} obtained via [Method 1](#); (Right) ψ_{21} computed using [Method 2](#).

Case 1: To identify the drift and diffusion function, we first use the value of ψ_{21} obtained via [Method 1](#) for the quadratic-coefficient SDE (31). The cross-validation heatmap and the CV curves in Fig. 16 reveal a broad near-flat basin of low validation error around $\alpha \sim 10^{-3}$ for moderate ρ . Using the 1-SE rule, the selected pair $(\alpha^\dagger, \rho^\dagger)$ lies within this stable region and is approximately

$$(\alpha^\dagger, \rho^\dagger) \approx (8.73 \times 10^{-4}, 0.50).$$

The δ -versus- n plots in Fig. 17 suggest sparse yet stable polynomial models with $n_\mu = 2$ and $n_\sigma = 2$ (the full-support choice for diffusion is larger). Thus, both the drift and diffusion blocks retain two active terms, and adding further terms does not yield a meaningful improvement in validation error. With these hyperparameters, the recovered functions are well captured by quadratic forms,

$$\hat{\mu}(x) = 0.620512x + 0.35905x^2, \quad \hat{\sigma}(x) = -0.0177782 + 0.535985x + 0.0842435x^2.$$

These estimates align with the intended polynomial structure, and the reconstructions of $\mu(X_t)$ and $\sigma(X_t)$ track the true curves closely; see Fig. 18(a)–(b). The overall fit remains strong with a small mean squared error $\text{MSE} = 1.448 \times 10^{-7}$. Moreover, the recovered noise follows the true driving noise well, and the path simulated using $\hat{\mu}$ and $\hat{\sigma}$ is almost indistinguishable from the observed trajectory; see Fig. 18(c)–(d). Overall, these results indicate that the method continues to recover the main dynamics reliably when ψ_{21} is obtained via regression, even in the presence of quadratic drift and diffusion structure.

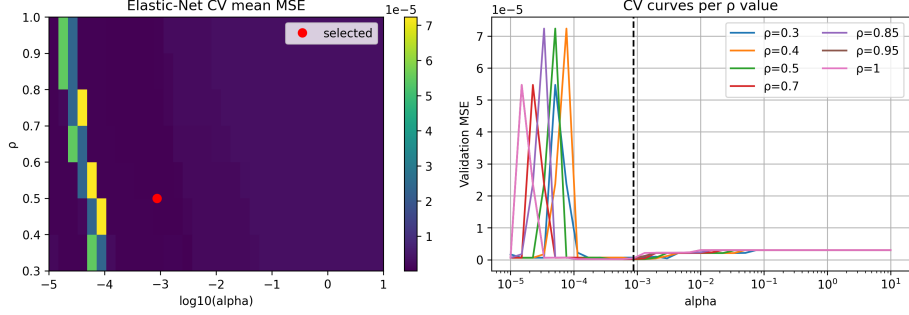


Figure 16: Time-series CV over (α, ρ) with de-biasing on the active set. The selected point $(\alpha^\dagger, \rho^\dagger) \approx (8.73 \times 10^{-4}, 0.50)$ lies in a broad near-optimal region.

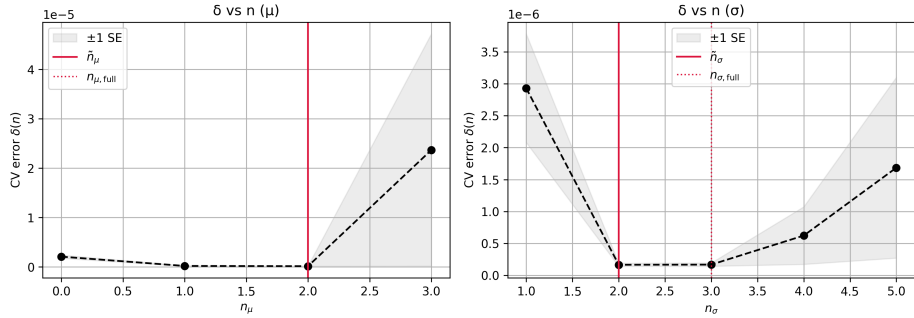


Figure 17: Validation error $\delta(n)$ versus support size n with ± 1 SE bands for the drift and diffusion blocks. The selected sizes are $n_\mu = 2$ and $n_\sigma = 2$, indicating sparse yet stable polynomial models.

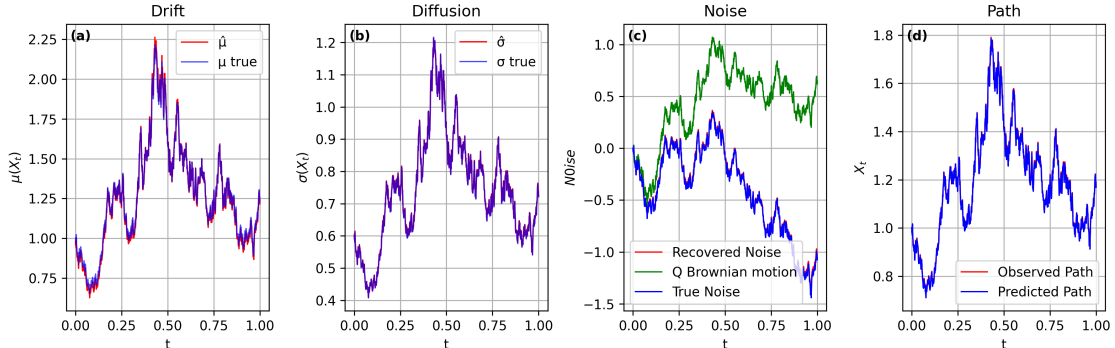


Figure 18: (a) True $\mu(X_t)$ and reconstructed $\hat{\mu}(X_t)$. (b) True $\sigma(X_t)$ and reconstructed $\hat{\sigma}(X_t)$. (c) True noise, recovered noise, and the \mathbb{Q} -Brownian motion. (d) Observed path X_t and the path simulated using the recovered $\hat{\mu}(X_t)$ and $\hat{\sigma}(X_t)$. Each vector is of length M with $M = 1000$.

Case 2: As a comparison to the first experiment, we repeat the same pipeline for the quadratic-coefficient SDE (31), but now we use the value of ψ_{21} computed using Method 2. The cross-validation heatmap and the CV curves in Fig. 19 again show a wide, almost flat region of low validation error. The selected hyperparameters fall inside this stable region and are approximately

$$(\alpha^\dagger, \rho^\dagger) \approx (8.73 \times 10^{-4}, 0.40),$$

which is of the same order as the regression-based choice. The δ -versus- n summaries in Fig. 20 select $n_\mu = 1$ and $n_\sigma = 2$, so the learned model remains sparse; adding more terms does not noticeably improve the CV error.

With this analytic ψ_{21} , the recovered drift and diffusion are

$$\hat{\mu}(x) = 1.02213 x, \quad \hat{\sigma}(x) = -0.0199718 + 0.540087 x + 0.0823874 x^2,$$

with mean squared error $\text{MSE} = 1.454 \times 10^{-7}$. Along the observed trajectory, the reconstructed $\mu(X_t)$ and $\sigma(X_t)$ follow the true curves closely (Fig. 21(a)–(b)). The recovered noise also aligns well with the true driving signal, and the path simulated under the learned model nearly overlaps the observed path (Fig. 21(c)–(d)). Overall, using the analytic ψ_{21} produces results consistent with the regression-based case, while keeping the identified model compact and stable.

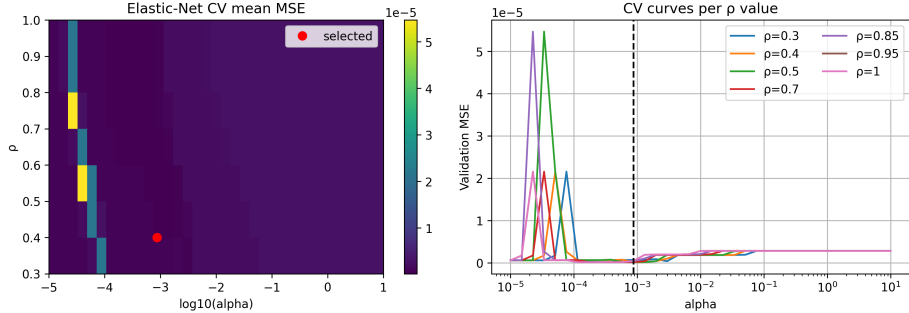


Figure 19: Time-series CV over (α, ρ) with de-biasing on the active set. The selected point $(\alpha^\dagger, \rho^\dagger) \approx (8.73 \times 10^{-4}, 0.40)$ lies in a broad near-optimal region.

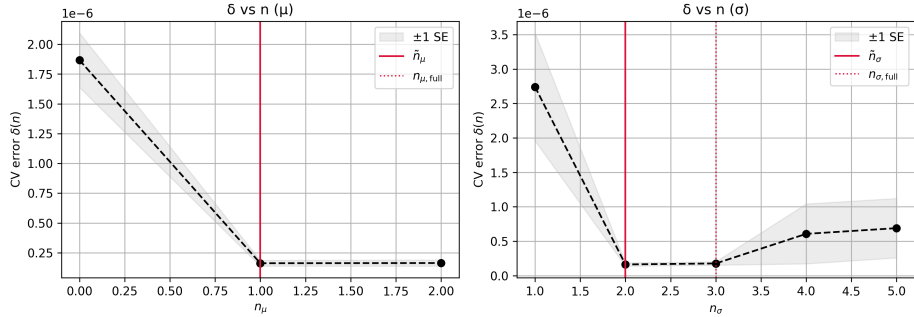


Figure 20: Validation error $\delta(n)$ versus support size n with ± 1 SE bands for the drift and diffusion blocks. The selected sparse sizes are $n_\mu = 1$ and $n_\sigma = 2$.

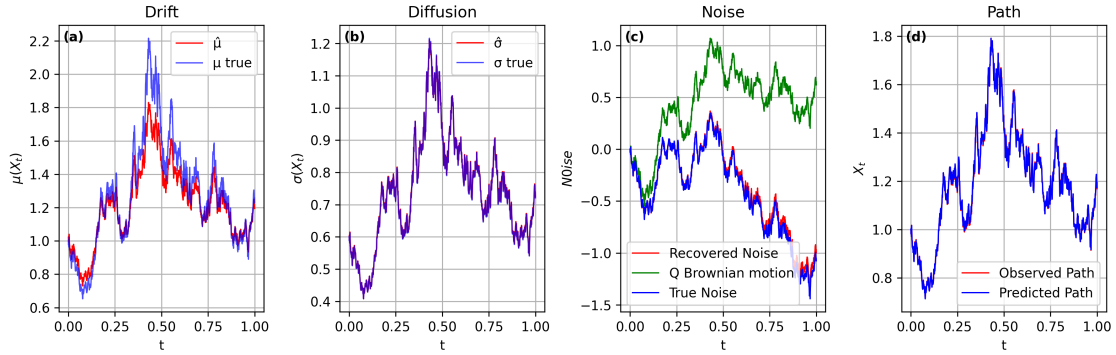


Figure 21: (a) True and recovered drift $\mu(X_t)$. (b) True and recovered diffusion $\sigma(X_t)$. (c) True noise, recovered noise, and the \mathbb{Q} -Brownian motion. (d) Observed and reconstructed paths of X_t . Each vector has length $M = 1000$.

5 Error analysis for Black-Scholes model

Proposition 5.1. *If X_t follows dynamic (8), and the data vector is observed at time grid $0 = t_0 < t_1 < \dots < t_N = T$. Denote $L^3(t)$ as the level-3 leading expansion term as in (22), then the approximation error of X_t for $t \in [0, T]$ in **Step 3** has the following estimate,*

$$\mathbb{P}\left(\sup_{t \in [t_k, t_{k+1}]} \|X_t - L^3(t)\| \geq \xi |t_{k+1} - t_k|^2; \tau < \zeta\right) \leq \exp\left(-\frac{c\xi^\alpha}{|t_{k+1} - t_k|}\right). \quad (32)$$

Furthermore, for $t \in [t_k, t_{k+1}]$, we have

$$\mathbb{E}[\|X_t - L^3(t)\|^2] \leq C |t_{k+1} - t_k|^2, \quad (33)$$

where C depends on the bound of μ, σ and their derivatives.

Corollary 5.2. *If X_t follows a Black-Scholes dynamics (30), and the data vector is observed at time grid $0 = t_0 < t_1 < \dots < t_N = T$, then the total approximation error of X_t for $t \in [0, T]$ has the following form,*

$$\mathbb{E}[\|X_t - L^3(t)\|^2] \leq C |t_{k+1} - t_k|^2, \quad (34)$$

where C depends on the bound of μ, σ and their derivatives.

References

- [1] Y. AïT-SAHALIA, *Maximum likelihood estimation of discretely sampled diffusions: A closed-form approximation approach*, *Econometrica*, 70 (2002), pp. 223–262.
- [2] A. ANANOVA AND R. CONT, *Pathwise integration with respect to paths of finite quadratic variation*, *Journal de Mathématiques Pures et Appliquées*, 107 (2017), pp. 737–757.
- [3] T. W. ANDERSON, *On asymptotic distributions of estimates of parameters of stochastic difference equations*, *The Annals of Mathematical Statistics*, 30 (1959), pp. 676–687.
- [4] I. P. ARRIBAS, *Derivatives pricing using signature payoffs*, arXiv preprint arXiv:1809.09466, (2018).
- [5] R. AZENCOTT, *Formule de taylor stochastique et développement asymptotique d'intégrales de feynmann*, in *Séminaire de Probabilités XVI*, LNM921, Springer, 1982, pp. 237–285.
- [6] Y. AÏT-SAHALIA, *Nonparametric pricing of interest rate derivative securities*, *Econometrica*, 64 (1996), pp. 527–560.
- [7] L. BACHELIER, *Théorie de la spéculation*, in *Annales scientifiques de l'École normale supérieure*, vol. 17, 1900, pp. 21–86.
- [8] Z. BAI, S. L. BRUNTON, B. W. BRUNTON, J. N. KUTZ, E. KAISER, A. SPOHN, AND B. R. NOACK, *Data-driven methods in fluid dynamics: Sparse classification from experimental data*, Springer, 2017.
- [9] C. BAYER, P. P. HAGER, S. RIEDEL, AND J. SCHOENMAKERS, *Optimal stopping with signatures*, *The Annals of Applied Probability*, 33 (2023), pp. 238–273.
- [10] B. M. BIBBY AND M. SØRENSEN, *Martingale estimation functions for discretely observed diffusion processes*, *Bernoulli*, (1995), pp. 17–39.
- [11] F. BLACK AND M. SCHOLES, *The pricing of options and corporate liabilities*, *Journal of political economy*, 81 (1973), pp. 637–654.
- [12] J. BONGARD AND H. LIPSON, *Automated reverse engineering of nonlinear dynamical systems*, *Proceedings of the National Academy of Sciences*, 104 (2007), pp. 9943–9948.
- [13] L. BONINSEGNA, F. NÜSKE, AND C. CLEMENTI, *Sparse learning of stochastic dynamical equations*, *The Journal of chemical physics*, 148 (2018).
- [14] S. L. BRUNTON, J. L. PROCTOR, AND J. N. KUTZ, *Discovering governing equations from data by sparse identification of nonlinear dynamical systems*, *Proceedings of the national academy of sciences*, 113 (2016), pp. 3932–3937.
- [15] G. CASELLA, M. GHOSH, J. GILL, AND M. KYUNG, *Penalized regression, standard errors, and Bayesian lassos*, *Bayesian Analysis*, 5 (2010), pp. 369 – 411.
- [16] F. CASTELL, *Asymptotic expansion of stochastic flows*, *Probability theory and related fields*, 96 (1993), pp. 225–239.
- [17] Z. CHEN, Y. LIU, AND H. SUN, *Physics-informed learning of governing equations from scarce data*, *Nature communications*, 12 (2021), p. 6136.

[18] F. COMTE, V. GENON-CATALOT, AND Y. ROZENHOLC, *Penalized nonparametric mean square estimation of the coefficients of diffusion processes*, Bernoulli, 13 (2007), pp. 514–543.

[19] C. CUCHIERO, G. GAZZANI, J. MÖLLER, AND S. SVALUTO-FERRO, *Joint calibration to spx and vix options with signature-based models*, Mathematical Finance, 35 (2025), pp. 161–213.

[20] C. CUCHIERO, G. GAZZANI, AND S. SVALUTO-FERRO, *Signature-based models: theory and calibration*, SIAM journal on financial mathematics, 14 (2023), pp. 910–957.

[21] D. DACUNHA-CASTELLE AND D. FLORENS-ZMIROU, *Estimation of the coefficients of a diffusion from discrete observations*, Stochastics: An International Journal of Probability and Stochastic Processes, 19 (1986), pp. 263–284.

[22] A. DALALYAN AND M. REISS, *Asymptotic statistical equivalence for ergodic diffusions: the multidimensional case*, Probability theory and related fields, 137 (2007), pp. 25–47.

[23] D. DAVYDOV AND V. LINETSKY, *Pricing and hedging path-dependent options under the cev process*, Management science, 47 (2001), pp. 949–965.

[24] D. DUFFIE AND P. GLYNN, *Estimation of continuous-time markov processes sampled at random time intervals*, Econometrica, 72 (2004), pp. 1773–1808.

[25] B. EFRON, T. HASTIE, I. JOHNSTONE, AND R. TIBSHIRANI, *Least angle regression*, The Annals of Statistics, 32 (2004), pp. 407–499.

[26] A. V. ERMOLAEV, A. SHEVELEVA, G. GENTY, C. FINOT, AND J. M. DUDLEY, *Data-driven model discovery of ideal four-wave mixing in nonlinear fibre optics*, Scientific Reports, 12 (2022), p. 12711.

[27] J. FAN AND C. ZHANG, *A reexamination of diffusion estimators with applications to financial model validation*, Journal of the American Statistical Association, 98 (2003), pp. 118–134.

[28] Q. FENG AND X. ZHANG, *Taylor expansions and castell estimates for solutions of stochastic differential equations driven by rough paths*, Journal of Stochastic Analysis, 1 (2020), p. 4.

[29] D. FLORENS-ZMIROU, *Approximate discrete-time schemes for statistics of diffusion processes*, Statistics: A Journal of Theoretical and Applied Statistics, 20 (1989), pp. 547–557.

[30] J. FRIEDMAN, T. HASTIE, AND R. TIBSHIRANI, *A note on the group lasso and a sparse group lasso*, arXiv preprint arXiv:1001.0736, (2010).

[31] P. K. FRIZ AND N. B. VICTOIR, *Multidimensional Stochastic Processes as Rough Paths: Theory and Applications*, Cambridge Studies in Advanced Mathematics, Cambridge University Press, 2010.

[32] I. V. GIRSANOV, *On transforming a certain class of stochastic processes by absolutely continuous substitution of measures*, Theory of Probability & Its Applications, 5 (1960), pp. 285–301.

[33] L. P. HANSEN AND J. A. SCHEINKMAN, *Back to the future: Generating moment implications for continuous-time markov processes*, 1993.

[34] L. P. HANSEN, J. A. SCHEINKMAN, AND N. TOUZI, *Spectral methods for identifying scalar diffusions*, Journal of Econometrics, 86 (1998), pp. 1–32.

[35] F. HARIRCHI, D. KIM, O. KHALIL, S. LIU, P. ELVATI, M. BARANWAL, A. HERO, AND A. VIOLI, *On sparse identification of complex dynamical systems: A study on discovering influential reactions in chemical reaction networks*, Fuel, 279 (2020), p. 118204.

[36] J. HARRISON AND S. R. PLISKA, *Martingales and stochastic integrals in the theory of continuous trading*, Stochastic Processes and their Applications, 11 (1981), pp. 215–260.

[37] T. HASTIE, R. TIBSHIRANI, J. FRIEDMAN, ET AL., *The elements of statistical learning*, 2009.

[38] A. A. KAPTANOGLU, C. HANSEN, J. D. LORE, M. LANDREMAN, AND S. L. BRUNTON, *Sparse regression for plasma physics*, Physics of Plasmas, 30 (2023).

[39] I. KARATZAS AND S. E. SHREVE, *Brownian Motion and Stochastic Calculus*, vol. 113 of Graduate Texts in Mathematics, Springer, New York, 2nd ed., 1991.

[40] M. KESSLER, *Estimation of an ergodic diffusion from discrete observations*, Scandinavian Journal of Statistics, 24 (1997), pp. 211–229.

[41] P. KIDGER AND T. LYONS, *Signatory: differentiable computations of the signature and logsignature transforms, on both cpu and gpu*, arXiv preprint arXiv:2001.00706, (2020).

[42] P. E. KLOEDEN AND E. PLATEN, *Stochastic Taylor Expansions*, Springer Berlin Heidelberg, Berlin, Heidelberg, 1992, pp. 161–226.

[43] J. R. KOZA, *Genetic programming as a means for programming computers by natural selection*, Statistics and computing, 4 (1994), pp. 87–112.

[44] Y. A. KUTOYANTS, *Statistical inference for ergodic diffusion processes*, Springer Science & Business Media, 2013.

[45] D. LAMOUROUX AND K. LEHNERTZ, *Kernel-based regression of drift and diffusion coefficients of stochastic processes*, Physics Letters A, 373 (2009), pp. 3507–3512.

[46] T. LYONS AND N. VICTOIR, *Cubature on wiener space*, Proceedings of the Royal Society of London. Series A: Mathematical, Physical and Engineering Sciences, 460 (2004), pp. 169–198.

[47] T. J. LYONS, *Differential equations driven by rough signals*, Revista Matemática Iberoamericana, 14 (1998), pp. 215–310.

[48] N. M. MANGAN, S. L. BRUNTON, J. L. PROCTOR, AND J. N. KUTZ, *Inferring biological networks by sparse identification of nonlinear dynamics*, IEEE Transactions on Molecular, Biological, and Multi-Scale Communications, 2 (2016), pp. 52–63.

[49] N. M. MANGAN, J. N. KUTZ, S. L. BRUNTON, AND J. L. PROCTOR, *Model selection for dynamical systems via sparse regression and information criteria*, Proceedings of the Royal Society A: Mathematical, Physical and Engineering Sciences, 473 (2017), p. 20170009.

[50] A. MELINO, *Estimation of continuous time models in finance*, Journal of Financial economics, 8 (1994), pp. 323–362.

[51] R. C. MERTON, *On estimating the expected return on the market: An exploratory investigation*, Journal of Financial Economics, 8 (1980), pp. 323–361.

[52] B. ØKSENDAL, *Stochastic differential equations*, in Stochastic differential equations: an introduction with applications, Springer, 2003, pp. 38–50.

[53] M. F. OSBORNE, *Brownian motion in the stock market*, Operations research, 7 (1959), pp. 145–173.

[54] S. H. RUDY, S. L. BRUNTON, J. L. PROCTOR, AND J. N. KUTZ, *Data-driven discovery of partial differential equations*, Science advances, 3 (2017), p. e1602614.

[55] H. SCHAEFFER, G. TRAN, AND R. WARD, *Learning dynamical systems and bifurcation via group sparsity*, arXiv preprint arXiv:1709.01558, (2017).

[56] M. SCHMIDT AND H. LIPSON, *Distilling free-form natural laws from experimental data*, science, 324 (2009), pp. 81–85.

[57] P. SEMNANI, V. GUAN, E. ROBEVA, AND D. LEE, *Path-dependent sdes: Solutions and parameter estimation*, 2025.

[58] R. STANTON, *A nonparametric model of term structure dynamics and the market price of interest rate risk*, The Journal of Finance, 52 (1997), pp. 1973–2002.

[59] J. M. STEVENS-HAAS, Y. BHANGALE, J. N. KUTZ, AND A. ARAVKIN, *Learning nonlinear dynamics using kalman smoothing*, IEEE Access, (2024).

[60] M. STONE, *Cross-validatory choice and assessment of statistical predictions*, Journal of the royal statistical society: Series B (Methodological), 36 (1974), pp. 111–133.

[61] S.-M. UDRESCU AND M. TEGMARK, *Ai feynman: A physics-inspired method for symbolic regression*, Science Advances, 6 (2020), p. eaay2631.

[62] M. WANNER AND I. MEZIĆ, *On higher order drift and diffusion estimates for stochastic sindy*, SIAM Journal on Applied Dynamical Systems, 23 (2024), pp. 1504–1539.

[63] M. YUAN AND Y. LIN, *Model selection and estimation in regression with grouped variables*, Journal of the Royal Statistical Society Series B: Statistical Methodology, 68 (2006), pp. 49–67.

[64] L. ZANNA AND T. BOLTON, *Data-driven equation discovery of ocean mesoscale closures*, Geophysical Research Letters, 47 (2020), p. e2020GL088376.

[65] S. ZHANG AND G. LIN, *Robust data-driven discovery of governing physical laws with error bars*, Proceedings of the Royal Society A: Mathematical, Physical and Engineering Sciences, 474 (2018), p. 20180305.

A Proof of Step 2

Recall that

$$\begin{aligned}
 X_t &= X_s + A_0(X_s) \int_s^t du + \int_s^t \int_s^u A'_0(X_r) \circ dX_r du + \sigma(X_s) \int_s^t \circ dB_u^{\mathbb{Q}} \\
 &\quad + \int_s^t \int_s^u \sigma'(X_r) \circ dX_r \circ dB_u^{\mathbb{Q}}.
 \end{aligned} \tag{35}$$

Plugging in the dynamics of dX_r 19 and applying the Taylor expansion at the starting point X_s , we get

$$\begin{aligned}
X_t &= X_s + A_0(X_s) \int_s^t du + \int_s^t \int_s^u A'_0(X_r)(A_0(X_r)dr + \sigma(X_r) \circ dB_r^Q)du \\
&\quad + \sigma(X_s) \int_s^t \circ dB_u^Q + \int_s^t \int_s^u \sigma'(X_r)(A_0(X_r)dr + \sigma(X_r) \circ dB_r^Q) \circ dB_u^Q \\
&= X_s + A_0(X_s) \int_s^t du + A'_0(X_s)A_0(X_s) \int_s^t \int_s^u dr du + A_0(X_s) \int_s^t du \\
&\quad + A'_0(X_s)\sigma(X_s) \int_s^t \int_s^u \circ dB_r^Q du \\
&\quad + \sigma(X_s) \int_s^t \circ dB_u^Q + \sigma'(X_s)A_0(X_s) \int_s^t \int_s^u dr \circ dB_u^Q \\
&\quad + \sigma'(X_s)\sigma(X_s) \int_s^t \int_s^u \circ dB_r^Q \circ dB_u^Q \\
&\quad + \int_s^t \int_s^u \int_s^r (A''_0(X_v)A_0(X_v) + A'_0(X_v)A'_0(X_v)) \circ dX_v dr \circ dB_u^Q \\
&\quad + \int_s^t \int_s^u \int_s^r (A''_0(X_v)\sigma(X_v) + A'_0(X_v)\sigma'(X_v)) \circ dX_v \circ dB_r^Q du \\
&\quad + \int_s^t \int_s^u \int_s^r (\sigma''(X_v)A_0(X_v) + \sigma'(X_v)A'_0(X_v)) \circ dX_v dr \circ dB_u^Q \\
&\quad + \int_s^t \int_s^u \int_s^r (\sigma''(X_v)\sigma(X_v) + \sigma'(X_v)\sigma'(X_v)) \circ dX_v \circ dB_r^Q \circ dB_u^Q
\end{aligned} \tag{36}$$

We collect higher order terms (i.e., with order equal or higher than $|t-s|^{2-\varepsilon}$, for any $\varepsilon > 0$, when $|t-s|$ is small) and denote them as the error term ε^{Ψ_2} . The leading term of $\int_s^t \int_s^u \int_s^r (\sigma''(X_v)\sigma(X_v) + \sigma'(X_v)\sigma'(X_v)) \circ dX_v \circ dB_r^Q \circ dB_u^Q$ will contribute one more $|t-s|^{3/2-\varepsilon}$ term, which has the following form,

$$(\sigma''(X_s)\sigma(X_s) + \sigma'(X_s)\sigma'(X_s)) \sigma(X_s) \int_s^t \int_s^u \int_s^r \circ dB_v^Q \circ dB_r^Q \circ dB_u^Q,$$

together with higher-order error terms. By collecting all the second-order iterated integrals, where the integral against Brownian motion has order $\frac{1}{2} - \varepsilon$, we end up with

$$\begin{aligned}
X_t &= X_s + \psi_1^{s,t} \int_s^t du + \psi_2^{s,t} \int_s^t dB_u + \psi_{12}^{s,t} \int_s^t \int_s^u dr \circ dB_u^Q \\
&\quad + \psi_{21}^{s,t} \int_s^t \int_s^u \circ dB_r^Q du + \psi_{22}^{s,t} \int_s^t \int_s^u \circ dB_r^Q \circ dB_u^Q \\
&\quad + \psi_{222}^{s,t} \int_s^t \int_s^u \int_s^r \circ dB_v^Q \circ dB_r^Q \circ dB_u^Q + \varepsilon^{\Psi_2},
\end{aligned}$$

where we denote $\Psi_2^{s,t} := \{\psi_1^{s,t}, \psi_2^{s,t}, \psi_{12}^{s,t}, \psi_{21}^{s,t}, \psi_{22}^{s,t}, \psi_{222}^{s,t}\}$ as the coefficients of the second order expansion of X_t , and $\varepsilon^{\Psi_2} (\approx |t-s|^{2-\varepsilon})$ as the error term for the second order expansion. The proof is thus completed. \square

B Proof of Step 3

Applying stochastic Taylor expansion on $\tilde{\mu}$ and σ around X_s , and truncating the Taylor expansion at level 2, we have the following approximation of $\tilde{\mu}$ and σ ,

$$\begin{aligned}
\tilde{\mu}(X_u) &= \tilde{\mu}(X_s) + \tilde{\mu}'(X_s) \int_s^u \circ dX_r + \tilde{\mu}''(X_s) \int_s^u \int_s^r \circ dX_v \circ dX_r \\
&\quad + \underbrace{\int_s^u \int_s^r \int_s^v \tilde{\mu}'''(\xi_\tau) \circ dX_\tau \circ dX_v \circ dX_r}_{\varepsilon^{\tilde{\mu}}}
\end{aligned} \tag{37}$$

$$\sigma(X_u) = \sigma(X_s) + \sigma'(X_s) \int_s^u \circ dX_r + \sigma''(X_s) \int_s^u \int_s^r \circ dX_v \circ dX_r \tag{38}$$

$$+ \underbrace{\int_s^u \int_s^r \int_s^v \sigma'''(\eta_\tau) \circ dX_\tau \circ dX_v \circ dX_r}_{\varepsilon^\sigma}$$

Where we denote $\varepsilon^{\tilde{\mu}}$ and ε^σ as the higher order approximation error wrt the second order expansion. Under some nominal Hölder assumptions on the underlying process X and smoothness of the functions $\tilde{\mu}$ and σ , these approximation errors of (37) and (38) are of order $|t_{i+1} - t_i|^{\frac{3}{2} - \varepsilon}$ on each time grid $[t_i, t_{i+1}]$. For clarity, we highlight the substitution of the expansion into the dynamics in blue. Substituting the second-order Taylor expansions (37) and (38) into (8) gives

$$\begin{aligned} X_t &= X_s + \int_s^t \left(\tilde{\mu}(X_s) + \tilde{\mu}'(X_s) \int_s^u \circ dX_r + \tilde{\mu}''(X_s) \int_s^u \int_s^r \circ dX_v \circ dX_r + \varepsilon^{\tilde{\mu}} \right) du \\ &\quad + \int_s^t \left(\sigma(X_s) + \sigma'(X_s) \int_s^u \circ dX_r + \sigma''(X_s) \int_s^u \int_s^r \circ dX_v \circ dX_r + \varepsilon^\sigma \right) \circ dB_u^{\mathbb{P}}. \end{aligned}$$

Plugging in dynamic (8) for dX_t in the above expansion, we get

$$\begin{aligned} X_t &= X_s + \tilde{\mu}(X_s) \int_s^t du + \sigma(X_s) \int_s^t \circ dB_u^{\mathbb{P}} \\ &\quad + \tilde{\mu}'(X_s) \int_s^t \int_s^u \left(\tilde{\mu}(X_r) dr + \sigma(X_r) \circ dB_r^{\mathbb{P}} \right) du \\ &\quad + \tilde{\mu}''(X_s) \int_s^t \int_s^u \int_s^r \left(\tilde{\mu}(X_v) dv + \sigma(X_v) \circ dB_v^{\mathbb{P}} \right) \left(\tilde{\mu}(X_r) dr + \sigma(X_r) \circ dB_r^{\mathbb{P}} \right) du \\ &\quad + \sigma'(X_s) \int_s^t \int_s^u \left(\tilde{\mu}(X_r) dr + \sigma(X_r) \circ dB_r^{\mathbb{P}} \right) \circ dB_u^{\mathbb{P}} \\ &\quad + \sigma''(X_s) \int_s^t \int_s^u \int_s^r \left(\tilde{\mu}(X_v) dv + \sigma(X_v) \circ dB_v^{\mathbb{P}} \right) \left(\tilde{\mu}(X_r) dr + \sigma(X_r) \circ dB_r^{\mathbb{P}} \right) \circ dB_u^{\mathbb{P}} \\ &\quad + \varepsilon^{\tilde{\mu}} \int_s^t ds + \varepsilon^\sigma \int_s^t \circ dB_u^{\mathbb{P}} \\ &= X_s + \tilde{\mu}(X_s) \int_s^t du + \sigma(X_s) \int_s^t \circ dB_u^{\mathbb{P}} + \tilde{\mu}'(X_s) \int_s^t \int_s^u \tilde{\mu}(X_r) dr du \\ &\quad + \tilde{\mu}'(X_s) \int_s^t \int_s^u \sigma(X_r) \circ dB_r^{\mathbb{P}} du + \sigma'(X_s) \int_s^t \int_s^u \tilde{\mu}(X_r) dr \circ dB_u^{\mathbb{P}} \\ &\quad + \sigma'(X_s) \int_s^t \int_s^u \tilde{\mu}(X_r) dr \circ dB_u^{\mathbb{P}} + \sigma'(X_s) \int_s^t \int_s^u \sigma(X_r) \circ dB_r^{\mathbb{P}} \circ dB_u^{\mathbb{P}} \\ &\quad + \tilde{\mu}''(X_s) \int_s^t \int_s^u \int_s^r \left(\tilde{\mu}(X_v) dv + \sigma(X_v) \circ dB_v^{\mathbb{P}} \right) \left(\tilde{\mu}(X_r) dr + \sigma(X_r) \circ dB_r^{\mathbb{P}} \right) du \\ &\quad + \sigma''(X_s) \int_s^t \int_s^u \int_s^r \left(\tilde{\mu}(X_v) dv + \sigma(X_v) \circ dB_v^{\mathbb{P}} \right) \left(\tilde{\mu}(X_r) dr + \sigma(X_r) \circ dB_r^{\mathbb{P}} \right) \circ dB_u^{\mathbb{P}} \\ &\quad + \varepsilon^{\tilde{\mu}} \int_s^t du + \varepsilon^\sigma \int_s^t \circ dB_u^{\mathbb{P}} \end{aligned}$$

For the double integral in the above expansion, apply first-order Taylor expansion for $\tilde{\mu}(X_r)$ and $\sigma(X_r)$ at X_s and plug in the dynamic for dX_t again, we further get

$$\begin{aligned} X_t &= X_s + \tilde{\mu}(X_s) \int_s^t du + \sigma(X_s) \int_s^t \circ dB_u^{\mathbb{P}} \\ &\quad + \tilde{\mu}'(X_s) \tilde{\mu}(X_s) \int_s^t \int_s^u dr du + \tilde{\mu}'(X_s) \sigma(X_s) \int_s^t \int_s^u \circ dB_r^{\mathbb{P}} du \\ &\quad + \sigma'(X_s) \tilde{\mu}(X_s) \int_s^t \int_s^u dr \circ dB_u^{\mathbb{P}} + \sigma'(X_s) \sigma(X_s) \int_s^t \int_s^u \circ dB_r^{\mathbb{P}} \circ dB_u^{\mathbb{P}} \\ &\quad + (\tilde{\mu}'(X_s))^2 \int_s^t \int_s^u \int_s^r \circ dX_v dr du + \tilde{\mu}'(X_s) \sigma'(X_s) \int_s^t \int_s^u \int_s^r \circ dX_v \circ dB_r^{\mathbb{P}} du \\ &\quad + \sigma'(X_s) \tilde{\mu}'(X_s) \int_s^t \int_s^u \int_s^r \circ dX_v dr \circ dB_u^{\mathbb{P}} \end{aligned}$$

$$\begin{aligned}
& + (\sigma'(X_s))^2 \int_s^t \int_s^u \int_s^r \circ dX_v \circ dB_r^\mathbb{P} \circ dB_u^\mathbb{P} \\
& + \tilde{\mu}''(X_s) \int_s^t \int_s^u \int_s^r (\tilde{\mu}(X_v) dv + \sigma(X_v) \circ dB_v^\mathbb{P}) (\tilde{\mu}(X_r) dr + \sigma(X_r) \circ dB_r^\mathbb{P}) du \\
& + \sigma''(X_s) \int_s^t \int_s^u \int_s^r (\tilde{\mu}(X_v) dv + \sigma(X_v) \circ dB_v^\mathbb{P}) (\tilde{\mu}(X_r) dr + \sigma(X_r) \circ dB_r^\mathbb{P}) \circ dB_u^\mathbb{P} \\
& + \varepsilon^{\tilde{\mu}} \int_s^t du + \varepsilon^\sigma \int_s^t \circ dB_u^\mathbb{P} \\
& = X_s + \tilde{\mu}(X_s) \int_s^t du + \sigma(X_s) \int_s^t \circ dB_u^\mathbb{P} + \tilde{\mu}'(X_s) \tilde{\mu}(X_s) \int_s^t \int_s^u dr du \\
& + \tilde{\mu}'(X_s) \sigma(X_s) \int_s^t \int_s^u \circ dB_r^\mathbb{P} du + \sigma'(X_s) \tilde{\mu}(X_s) \int_s^t \int_s^u dr \circ dB_u^\mathbb{P} \\
& + \sigma'(X_s) \sigma(X_s) \int_s^t \int_s^u \circ dB_r^\mathbb{P} \circ dB_u^\mathbb{P} \\
& + (\tilde{\mu}'(X_s))^2 \int_s^t \int_s^u \int_s^r (\tilde{\mu}(X_v) dv + \sigma(X_v) \circ dB_v^\mathbb{P}) dr du \\
& + \tilde{\mu}'(X_s) \sigma'(X_s) \int_s^t \int_s^u \int_s^r (\tilde{\mu}(X_v) dv + \sigma(X_v) \circ dB_v^\mathbb{P}) \circ dB_r^\mathbb{P} du \\
& + \sigma'(X_s) \tilde{\mu}'(X_s) \int_s^t \int_s^u \int_s^r (\tilde{\mu}(X_v) dv + \sigma(X_v) \circ dB_v^\mathbb{P}) dr \circ dB_u^\mathbb{P} \\
& + (\sigma'(X_s))^2 \int_s^t \int_s^u \int_s^r (\tilde{\mu}(X_v) dv + \sigma(X_v) \circ dB_v^\mathbb{P}) \circ dB_r^\mathbb{P} \circ dB_u^\mathbb{P} \\
& + \tilde{\mu}''(X_s) \int_s^t \int_s^u \int_s^r (\tilde{\mu}(X_v) dv + \sigma(X_v) \circ dB_v^\mathbb{P}) (\tilde{\mu}(X_r) dr + \sigma(X_r) \circ dB_r^\mathbb{P}) du \\
& + \sigma''(X_s) \int_s^t \int_s^u \int_s^r (\tilde{\mu}(X_v) dv + \sigma(X_v) \circ dB_v^\mathbb{P}) (\tilde{\mu}(X_r) dr + \sigma(X_r) \circ dB_r^\mathbb{P}) \circ dB_u^\mathbb{P} \\
& + \varepsilon^{\tilde{\mu}} \int_s^t du + \varepsilon^\sigma \int_s^t \circ dB_u^\mathbb{P}
\end{aligned}$$

Finally, replacing $\tilde{\mu}$ and σ with their Taylor expansion around X_s and combining the like terms up to triple integrals, gives the following expansion

$$\begin{aligned}
X_t & = X_s + \tilde{\mu}(X_s) \int_s^t du + \sigma(X_s) \int_s^t \circ dB_u^\mathbb{P} + \tilde{\mu}'(X_s) \tilde{\mu}(X_s) \int_s^t \int_s^u dr du \\
& + \tilde{\mu}'(X_s) \sigma(X_s) \int_s^t \int_s^u \circ dB_r^\mathbb{P} du + \sigma'(X_s) \tilde{\mu}(X_s) \int_s^t \int_s^u dr \circ dB_u^\mathbb{P} \\
& + \sigma'(X_s) \sigma(X_s) \int_s^t \int_s^u \circ dB_r^\mathbb{P} \circ dB_u^\mathbb{P} \\
& + ((\tilde{\mu}'(X_s))^2 \tilde{\mu}(X_s) + \tilde{\mu}''(X_s) (\tilde{\mu}(X_s))^2) \int_s^t \int_s^u \int_s^r dv dr du \\
& + ((\tilde{\mu}'(X_s))^2 \sigma(X_s) + \tilde{\mu}''(X_s) \tilde{\mu}(X_s) \sigma(X_s)) \int_s^t \int_s^u \int_s^r \circ dB_v^\mathbb{P} dr du \\
& + (\tilde{\mu}'(X_s) \sigma'(X_s) \tilde{\mu}(X_s) + \tilde{\mu}''(X_s) \tilde{\mu}(X_s) \sigma(X_s)) \int_s^t \int_s^u \int_s^r dv \circ dB_r^\mathbb{P} du \\
& + (\tilde{\mu}'(X_s) \sigma'(X_s) \tilde{\mu}(X_s) + \sigma''(X_s) (\tilde{\mu}(X_s))^2) \int_s^t \int_s^u \int_s^r dv dr \circ dB_u^\mathbb{P} \\
& + (\tilde{\mu}'(X_s) \sigma'(X_s) \sigma(X_s) + \tilde{\mu}''(X_s) (\sigma(X_s))^2) \int_s^t \int_s^u \int_s^r \circ dB_v^\mathbb{P} \circ dB_r^\mathbb{P} du \\
& + (\tilde{\mu}'(X_s) \sigma'(X_s) \sigma(X_s) + \sigma''(X_s) \sigma(X_s) \tilde{\mu}(X_s)) \int_s^t \int_s^u \int_s^r \circ dB_v^\mathbb{P} dr \circ dB_u^\mathbb{P} \\
& + ((\sigma'(X_s))^2 \tilde{\mu}(X_s) + \sigma''(X_s) \sigma(X_s) \tilde{\mu}(X_s)) \int_s^t \int_s^u \int_s^r dv \circ dB_r^\mathbb{P} \circ dB_u^\mathbb{P} \\
& + ((\sigma'(X_s))^2 \sigma(X_s) + \sigma''(X_s) (\sigma(X_s))^2) \int_s^t \int_s^u \int_s^r \circ dB_v^\mathbb{P} \circ dB_r^\mathbb{P} \circ dB_u^\mathbb{P}
\end{aligned}$$

$$+ \underbrace{\varepsilon^{\tilde{\mu}} \int_s^t du + \varepsilon^\sigma \int_s^t \circ dB_u^{\mathbb{P}} + \tilde{\varepsilon}^{\tilde{\mu}, \sigma}}_{:= \varepsilon^{\tilde{\mu}, \sigma}}, \quad (39)$$

where we denote $\tilde{\varepsilon}^{\tilde{\mu}, \sigma}$ as the collection of all the higher order error terms from double and triple integrals. We denote $\varepsilon^{\tilde{\mu}, \sigma} := \varepsilon^{\tilde{\mu}} \int_0^t ds + \varepsilon^\sigma \int_0^t \circ dB_s^{\mathbb{P}} + \tilde{\varepsilon}^{\tilde{\mu}, \sigma}$ as the overall error term from the above expansion. This completes the proof. \square

C Proof of Step 4

Applying Girsanov theorem, plugging the dynamic $dB_t^{\mathbb{P}} = dB_t^{\mathbb{Q}} - \frac{\mu(X_t)}{\sigma(X_t)}dt$ into the expansion (39) from Step 3, we have

$$\begin{aligned} X_t &= X_s + \tilde{\mu}(X_s) \int_s^t du + \sigma(X_s) \int_s^t \circ \left(dB_u^{\mathbb{Q}} - \frac{\mu(X_u)}{\sigma(X_u)} du \right) \\ &\quad + \tilde{\mu}'(X_s) \tilde{\mu}(X_s) \int_s^t \int_s^u dr du + \tilde{\mu}'(X_s) \sigma(X_s) \int_s^t \int_s^u \circ \left(dB_r^{\mathbb{Q}} - \frac{\mu(X_r)}{\sigma(X_r)} dr \right) du \\ &\quad + \sigma'(X_s) \tilde{\mu}(X_s) \int_s^t \int_s^u dr \circ \left(dB_u^{\mathbb{Q}} - \frac{\mu(X_u)}{\sigma(X_u)} du \right) \\ &\quad + \sigma'(X_s) \sigma(X_s) \int_s^t \int_s^u \circ \left(dB_r^{\mathbb{Q}} - \frac{\mu(X_r)}{\sigma(X_r)} dr \right) \circ \left(dB_u^{\mathbb{Q}} - \frac{\mu(X_u)}{\sigma(X_u)} du \right) \\ &\quad + ((\tilde{\mu}'(X_s))^2 \tilde{\mu}(X_s) + \tilde{\mu}''(X_s)(\tilde{\mu}(X_s))^2) \int_s^t \int_s^u \int_s^r dv dr du \\ &\quad + ((\tilde{\mu}'(X_s))^2 \sigma(X_s) + \tilde{\mu}''(X_s) \tilde{\mu}(X_s) \sigma(X_s)) \\ &\quad \quad \times \int_s^t \int_s^u \int_s^r \circ \left(dB_v^{\mathbb{Q}} - \frac{\mu(X_v)}{\sigma(X_v)} dv \right) dr du \\ &\quad + (\tilde{\mu}'(X_s) \sigma'(X_s) \tilde{\mu}(X_s) + \tilde{\mu}''(X_s) \tilde{\mu}(X_s) \sigma(X_s)) \\ &\quad \quad \times \int_s^t \int_s^u \int_s^r dv \circ \left(dB_r^{\mathbb{Q}} - \frac{\mu(X_r)}{\sigma(X_r)} dr \right) du \\ &\quad + (\tilde{\mu}'(X_s) \sigma'(X_s) \tilde{\mu}(X_s) + \sigma''(X_s)(\tilde{\mu}(X_s))^2) \\ &\quad \quad \int_s^t \int_s^u \int_s^r dv dr \circ \left(dB_u^{\mathbb{Q}} - \frac{\mu(X_u)}{\sigma(X_u)} du \right) \\ &\quad + (\tilde{\mu}'(X_s) \sigma'(X_s) \sigma(X_s) + \tilde{\mu}''(X_s)(\sigma(X_s))^2) \\ &\quad \quad \times \int_s^t \int_s^u \int_s^r \circ \left(dB_v^{\mathbb{Q}} - \frac{\mu(X_v)}{\sigma(X_v)} dv \right) \circ \left(dB_r^{\mathbb{Q}} - \frac{\mu(X_r)}{\sigma(X_r)} dr \right) du \\ &\quad + (\tilde{\mu}'(X_s) \sigma'(X_s) \sigma(X_s) + \sigma''(X_s) \sigma(X_s) \tilde{\mu}(X_s)) \\ &\quad \quad \times \int_s^t \int_s^u \int_s^r \circ \left(dB_v^{\mathbb{Q}} - \frac{\mu(X_v)}{\sigma(X_v)} dv \right) dr \circ \left(dB_u^{\mathbb{Q}} - \frac{\mu(X_u)}{\sigma(X_u)} du \right) \\ &\quad + ((\sigma'(X_s))^2 \tilde{\mu}(X_s) + \sigma''(X_s) \sigma(X_s) \tilde{\mu}(X_s)) \\ &\quad \quad \times \int_s^t \int_s^u \int_s^r dv \circ \left(dB_r^{\mathbb{Q}} - \frac{\mu(X_r)}{\sigma(X_r)} dr \right) \circ \left(dB_u^{\mathbb{Q}} - \frac{\mu(X_u)}{\sigma(X_u)} du \right) \\ &\quad + ((\sigma'(X_s))^2 \sigma(X_s) + \sigma''(X_s)(\sigma(X_s))^2) \\ &\quad \quad \times \int_s^t \int_s^u \int_s^r \circ \left(dB_v^{\mathbb{Q}} - \frac{\mu(X_v)}{\sigma(X_v)} dv \right) \circ \left(dB_r^{\mathbb{Q}} - \frac{\mu(X_r)}{\sigma(X_r)} dr \right) \circ \left(dB_u^{\mathbb{Q}} - \frac{\mu(X_u)}{\sigma(X_u)} du \right) \\ &\quad + \underbrace{\varepsilon^{\tilde{\mu}} \int_s^t du + \varepsilon^\sigma \int_s^t \circ dB_u^{\mathbb{P}} + \tilde{\varepsilon}^{\tilde{\mu}, \sigma}}_{:= \varepsilon^{\tilde{\mu}, \sigma}}, \end{aligned} \quad (40)$$

Note that for the Black-Scholes model, the linear constant drift and diffusion coefficient assumption ensures that $\frac{\mu(X_u)}{\sigma(X_u)} = \frac{\mu(X_s)}{\sigma(X_s)}$ for all $u \in [s, t)$. In the spirit of Black-Scholes, we propose further approximation of $\frac{\mu(X_u)}{\sigma(X_u)}$ by $\frac{\mu(X_s)}{\sigma(X_s)}$ for the interval $[s, t)$, and we denote $\varepsilon^{\mu/\sigma}$ as the error term from this approximation. This ensures some cancellations. Higher approximations of $\frac{\mu(X_u)}{\sigma(X_u)}$ is also possible here; we leave this for future studies. To derive the third-order approximation, we only collect the integrals with order $|t - s|^{3/2}$ terms in the above expansion, leaving all the higher terms in the error term. With a slight abuse of notation, we denote by $\varepsilon^{\tilde{\mu}, \sigma}$ the

error term associated with the Taylor expansion for functions $\tilde{\mu}$ and σ , and by $\varepsilon^{\mu/\sigma}$ the error term associated with the approximation for $\frac{\mu}{\sigma}$. The final result after truncating to a third-order iterated integral and replacing $\frac{\mu(X_u)}{\sigma(X_u)}$ by the starting point $\frac{\mu(X_s)}{\sigma(X_s)}$ will be as follows.

$$\begin{aligned}
X_t &= X_s - \frac{1}{2}\sigma(X_s)\sigma'(X_s) \int_s^t du + \sigma(X_s) \int_s^t \circ dB_u^{\mathbb{Q}} \\
&\quad + \left(\mu'(X_s)\sigma(X_s) - \mu(X_s)\sigma'(X_s) - \frac{1}{2}\sigma(X_s)\sigma'(X_s)^2 - \frac{1}{2}\sigma(X_s)^2\sigma''(X_s) \right) \\
&\quad \times \int_s^t \int_s^u \circ dB_r^{\mathbb{Q}} du \\
&\quad - \frac{1}{2}\sigma(X_s)\sigma'(X_s)^2 \int_0^t \int_0^s du \circ dB_s^{\mathbb{Q}} + \sigma'(X_s)\sigma(X_s) \int_s^t \int_s^u \circ dB_r^{\mathbb{Q}} \circ dB_u^{\mathbb{Q}} \\
&\quad + ((\sigma'(X_s))^2\sigma(X_s) + \sigma''(X_s)(\sigma(X_s))^2) \int_s^t \int_s^u \int_s^r \circ dB_v^{\mathbb{Q}} \circ dB_r^{\mathbb{Q}} \circ dB_u^{\mathbb{Q}} \\
&\quad + \varepsilon^{\tilde{\mu}, \sigma} + \varepsilon^{\mu/\sigma}.
\end{aligned}$$

The overall error terms $\varepsilon^{\tilde{\mu}, \sigma} + \varepsilon^{\mu/\sigma}$ has the same order as $|t-s|^{2-\varepsilon}$, which is small if $|t-s|$ is small. The proof is thus finished. \square

D Proof of Step 5

Comparing the coefficients of (20) from Step 2 and (23) from Step 4, for the expansion of X_t at the initial point X_s on interval $[s, t)$, we have the following equalities,

$$\begin{cases} -\frac{1}{2}\sigma(X_s)\sigma'(X_s) = \psi_1^{s,t}, & \sigma(X_s) = \psi_2^{s,t}, & -\frac{1}{2}\sigma(X_s)\sigma'(X_s)^2 = \psi_{12}^{s,t} \\ \mu'(X_s)\sigma(X_s) - \mu(X_s)\sigma'(X_s) - \frac{1}{2}\sigma(X_s)\sigma'(X_s)^2 - \frac{1}{2}\sigma(X_s)^2\sigma''(X_s) = \psi_{21}^{s,t}, \\ \sigma(X_s)\sigma'(X_s) = \psi_{22}^{s,t}. \end{cases} \quad (41)$$

As we already get the values/functions of σ from step 1, we only focus on the function μ here. The equation associated with $\psi_{21}^{s,t}$ implies that

$$\mu'(X_s)\sigma(X_s) - \mu(X_s)\sigma'(X_s) - \frac{1}{2}\sigma(X_s)\sigma'(X_s)^2 - \frac{1}{2}\sigma(X_s)^2\sigma''(X_s) = \psi_{21}^{s,t}. \quad (42)$$

Following the above observation, the parameter $\psi_{21}^{t_i, t_{i+1}}$ can be found corresponding to the initial value X_{t_i} , for $i = 0, 1, 2, \dots, n$. With this, the equation (42) holds true for each t_i , $i = 0, 1, 2, \dots, n$. For example, (42) is equivalently written as

$$\mu'(X_{t_i})\sigma(X_{t_i}) - \mu(X_{t_i})\sigma'(X_{t_i}) - \frac{1}{2}\sigma(X_{t_i})\sigma'(X_{t_i})^2 - \frac{1}{2}\sigma(X_{t_i})^2\sigma''(X_{t_i}) = \psi_{21}^{t_i, t_{i+1}}, \quad (43)$$

$$\forall i = 0, 1, 2, \dots, n.$$

Denote $a(X_r) = \frac{\sigma'(X_r)}{\sigma(X_r)}$ and $b(X_r) = \frac{2\psi_{21}^{t_i, t_{i+1}} + \sigma(X_r)\sigma'(X_r)^2 + \sigma(X_r)^2\sigma''(X_r)}{2\sigma(X_r)}$, for $r \in [t_i, t_{i+1})$. Since we know $\mu(X_0)$, using Eular scheme for each interval $[t_i, t_{i+1})$, we can solve μ as follows

$$\mu(X_{t_i}) = \mu(X_{t_{i-1}}) + [a(X_{t_{i-1}})\mu(X_{t_{i-1}}) + b(X_{t_{i-1}})](X_{t_i} - X_{t_{i-1}}), \quad \forall i = 1, 2, \dots, n. \quad (44)$$

Thus, we use estimate the values of $\mu(X_{t_i})$ for $i = 1, \dots, N$. The proof is thus finished. \square

E Proof of Proposition 5.1

The expansion of X_t in **Step 3** is a Taylor expansion for the following SDE,

$$X_t = X_s + \int_s^t V_0(X_r)dr + \int_s^t V_1(X_r) \circ dB_r^{\mathbb{P}}, \quad (45)$$

where we denote the vector field $V_0(X_r) = \tilde{\mu}(X_r)$, and $V_1(X_r) = \sigma(X_r)$ to simplify the notation. According to [5, Theorem 1.6] (see also [28, Lemma 3.9] for a more general set-up of this expansion), for the one dimensional X_t , we have

$$X_t = X_s + \sum_{k=1}^N g_k(t, s) + |t-s|^{\frac{N+1}{2}} R^{N+1}(t, s), \quad (46)$$

where we set $\mathbf{B}_t^0 = t$, and $\mathbf{B}_t^1 = B_t^{\mathbb{P}}$, and introduce the following notation,

$$g_k(t, s) = \sum_{|I|=k} P_I(X_s) \int_{s < t_1 < t_2 \cdots < t_k < t} \circ d\mathbf{B}_{t_1}^{i_1} \cdots \circ d\mathbf{B}_{t_k}^{i_k}, \quad (47)$$

for a word $I = (i_1, \dots, i_k) \in \{0, 1\}^k$. Here we denote $|I|$ the size of I which equals k , and we denote $P_I(X_s) = (V_{i_1} \cdots V_{i_k})(X_s)$. In particular, $V_{i_1} \cdots V_{i_k} := (V_{i_1} \cdots (V_{i_{k-2}}(V_{i_{k-1}}V_{i_k})) \cdots)$ represents the iterative operation of the vector fields in order. Following from [5, Proposition 4.3] (see also [28, Lemma 3.9] with $H = 1/2$), there exists a random time ζ , some constants $\alpha, c > 0$, for every $\xi \geq 1$, such that

$$\begin{aligned} \mathbb{P} \left(\sup_{t \in [t_k, t_{k+1}]} \| |t - t_k|^{\frac{N+1}{2}} R_{m+1}(t, t_k) \| \geq \xi |t_{k+1} - t_k|^{\frac{N+1}{2}}; \tau < \zeta \right) \\ \leq \exp \left(- \frac{c \xi^\alpha}{|t_{k+1} - t_k|} \right). \end{aligned}$$

The random time ζ is the exit time of X_t in a compact domain K . We pick the compact domain K large enough, such that X_t stays inside K for $t \in [t_k, t_{k+1}]$. Since we take the Taylor expansion at level 3, by selecting $N = 3$, we have

$$\mathbb{P} \left(\sup_{t \in [t_k, t_{k+1}]} \| R_{m+1}(t, t_k) \| \geq \xi |t_{k+1} - t_k|^2; \tau < \zeta \right) \leq \exp \left(- \frac{c \xi^\alpha}{|t_{k+1} - t_k|} \right).$$

Applying the above estimate, denote $Z = \|X_t - L^3(t)\|^2$, where $L^3(t) = X_{t_k} + \sum_{k=1}^3 g_k(t, t_k)$ as defined in (46), we have

$$\mathbb{E}[\|X_t - L^3(t)\|^2] = \mathbb{E}[Z] = \int_0^\infty \mathbb{P}(Z > z) dz \leq C |t_{k+1} - t_k|^2,$$

which completes the proof.

F Proof of Corollary 5.2

First, recall that the total approximation error of X_t accumulated from **Step 1-3** is coming from the error terms $\varepsilon^{\tilde{\mu}}$, ε^σ , $\varepsilon^{\tilde{\mu}, \sigma}$ and $\varepsilon^{\mu/\sigma}$. For the Black-Scholes model since $\sigma(X_t) = \sigma X_t$ and $\tilde{\mu}(X_t) = \mu X_t - \sigma^2 X_t$, the Equations (37) and (38) simplifies to

$$\begin{aligned} \tilde{\mu}(X_u) &= \tilde{\mu}(X_s) + (\mu - \sigma^2) \int_s^u \circ dX_r + 0 \\ \sigma(X_u) &= \sigma(X_s) + \sigma^2 \int_s^u \circ dX_r + 0. \end{aligned}$$

This implies $\varepsilon^{\tilde{\mu}} = \varepsilon^\sigma = 0$ in **Step 2**. Furthermore, $\frac{\mu(X_s)}{\sigma(X_s)} = \frac{\mu}{\sigma}$, we get $\varepsilon^{\mu/\sigma} = 0$ in **Step 4**. Thus, we only need to estimate the error X_t in **Step 3**, the proof follows directly from Proposition 5.1.